



Recent Collider Physics Results from DØ

H. Eugene Fisk

for the DØ Experiment

550 collaborators from 18 nations;

90 institutes = 39 US, 51 non-US



Short History

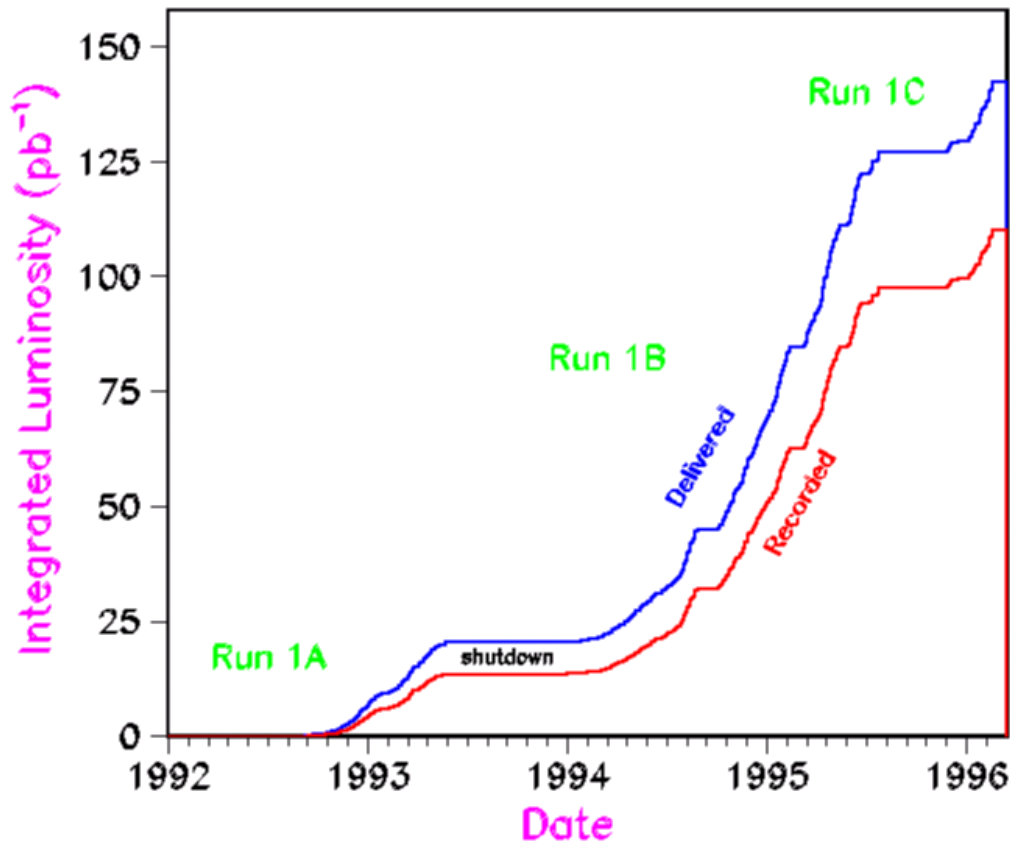
- The TeVatron SC accelerator - 1983
- Decision: 2nd collider experiment - 1984
- Expected luminosity: $10^{30} \text{ cm}^{-2}\text{sec}^{-1}$
- Technology: Measure leptons/jets
- Central tracking drift chambers; LAr/U EM & Had. calorimeters, Muons: Fe toroids
- DØ Exp'l area 1986; detector construction until 1991; Run 1: '92 - '96.

CDF/DØ Top Discovery in 1995



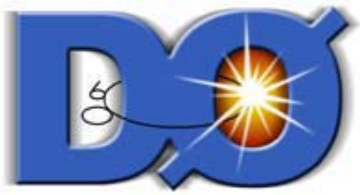
DØ Run 1 Integrated Luminosity

DØ Run 1 Integrated Luminosity



From the DØ Design Report 11/84:
“In the face of expected results from CERN ...will need $L = 10^{30} \text{cm}^{-2} \text{sec}^{-1}$ and 50% efficiency over four months to obtain 5pb^{-1} ”.

Once running did $\sim 14 \text{pb}^{-1}$ in 6 months with good efficiency.



LAr/U Calorimetry

Why LAr and U?

U has high density, which was desired because space was very limited in 1984; the Main Ring was in the tunnel about 25 " above the Tevatron. "Not another bypass like CDF".

LAr provided the opportunity for: uniform gain, variable cal cell sizes, ganging of cells to make towers, cold temperature that implied low det. noise.

Gap sig. $\sim 50K$ e's; (dE/dx) noise $\sim 10K$ e's + U noise

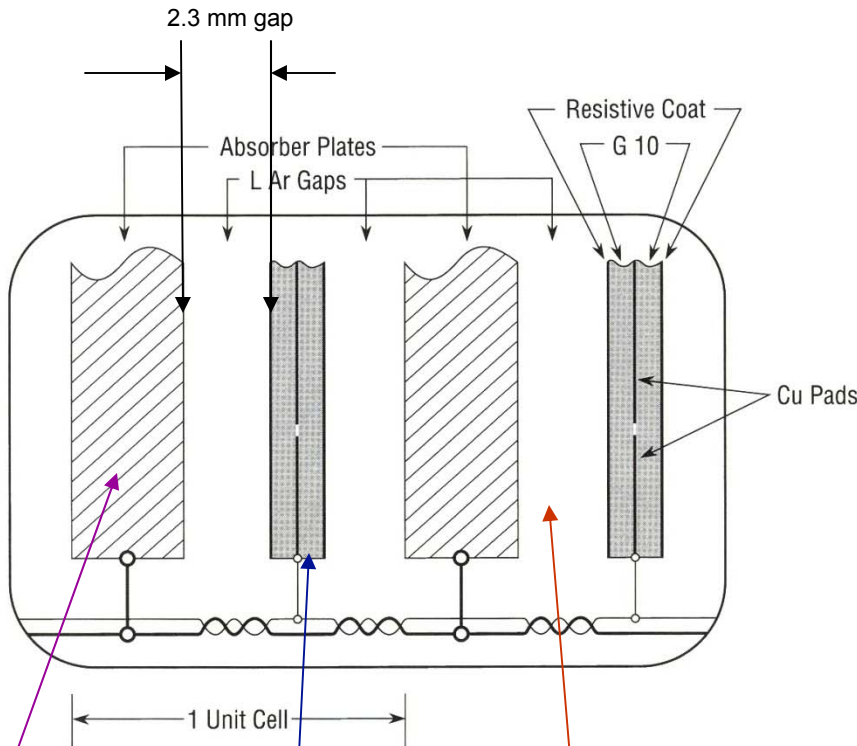


Fig. 27. Schematic view of the liquid argon gap and signal board unit cell.

U-plate
4/6 mm

Signal
board

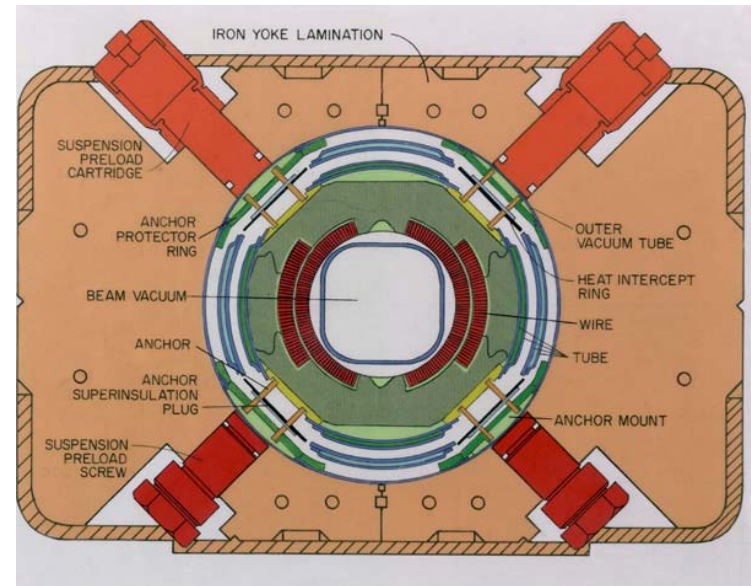
Filled
w/LAr



DØ's Ingredients for Success



The Fermilab Tevatron
The DØ Collaboration
The DØ Detector
Fermilab management
US and International Support





DØ Jet Definition

Invariant Cross section:

$$E \frac{d^3 \sigma}{dp^3} \rightarrow \frac{d^3 \sigma}{dy dp_{\perp}^2}$$

$$\text{Rapidity } y = \frac{1}{2} \ln \left(\frac{E + P_z}{E - P_z} \right)$$

becomes pseudo-rapidity:

$$\eta = -\ln \left(\tan \frac{\theta}{2} \right) \text{ for masses } \approx 0$$

DØ jets are often defined within a cone of radius $R = 0.7$ in pseudo-rapidity η and azimuthal angle ϕ .

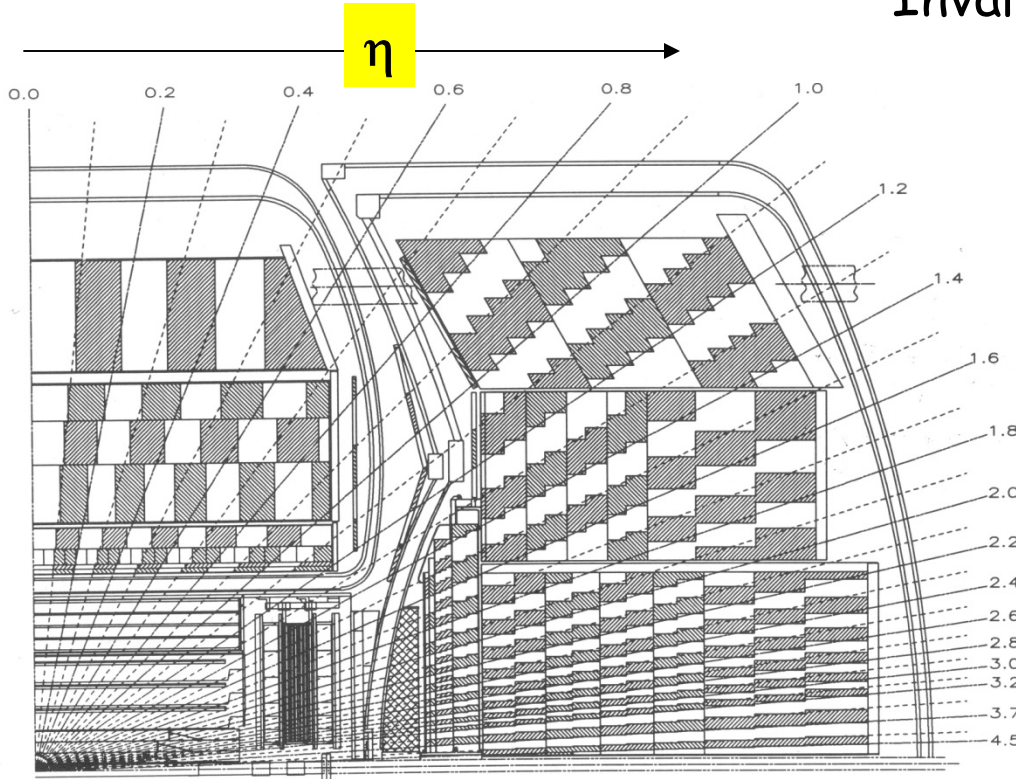
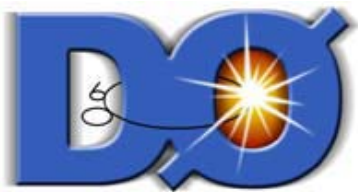


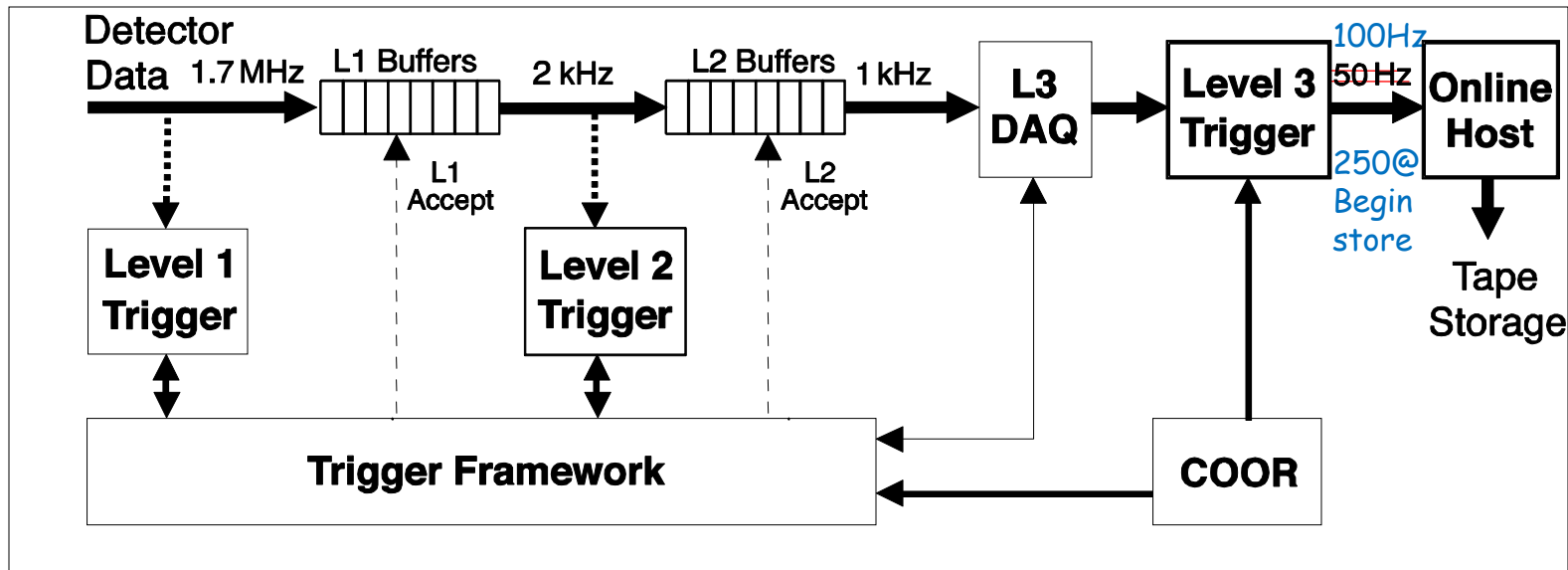
Fig. 28. Schematic view of a portion of the DØ calorimeters showing the transverse and longitudinal segmentation pattern. The shading pattern indicates the distinct cells for signal readout. The rays indicate the pseudorapidity intervals seen from the center of the detector.

The tower structure is useful for defining jets. It is also useful for filtering events, since the event rate is too large to take all events.

Rate = $\sigma \times L$; $L \sim 10^{32} \text{ cm}^{-2}\text{sec}^{-1}$; $\sigma_{\text{tot}} \sim 70\text{mb}$. Homework! How to filter?



DØ's Three Level Trigger



L1: Hardware

- Calor. Tower E_T 's
- Missing E_T , $\sum |E_T|$
- p_T Trk patterns for μ , Central-Fiber Tracks.
- CFT/CPS clusters;
- Pre-scales applied to low E_T , p_T triggers.

L2: PC/VME boards

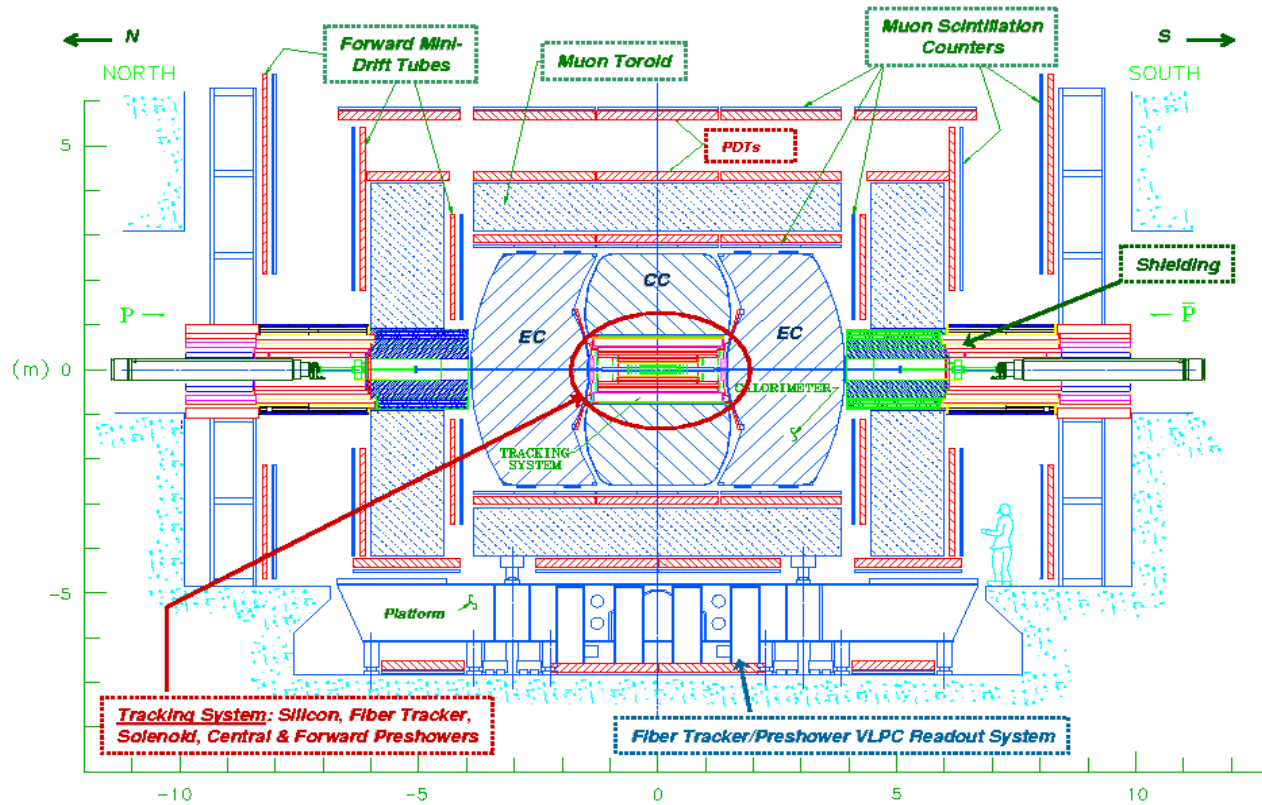
- Run software algorithms w/L1 readout geometry.
- Match trigger objects between sub-systems.
- Reduce rate by 2.

L3: PC Farm Nodes using a version of off-line code.

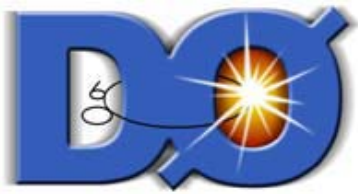
- Analyze full events
- Cuts using multiple detectors, multiple objects.
- Reduce event rate by a factor of 10 or more.



DØ Run II Upgrades

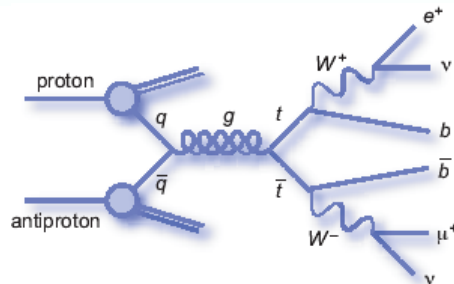
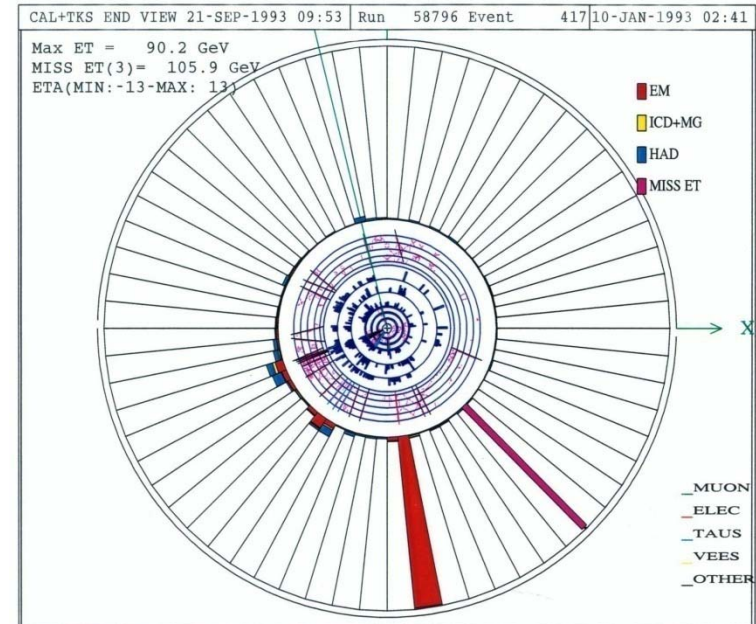
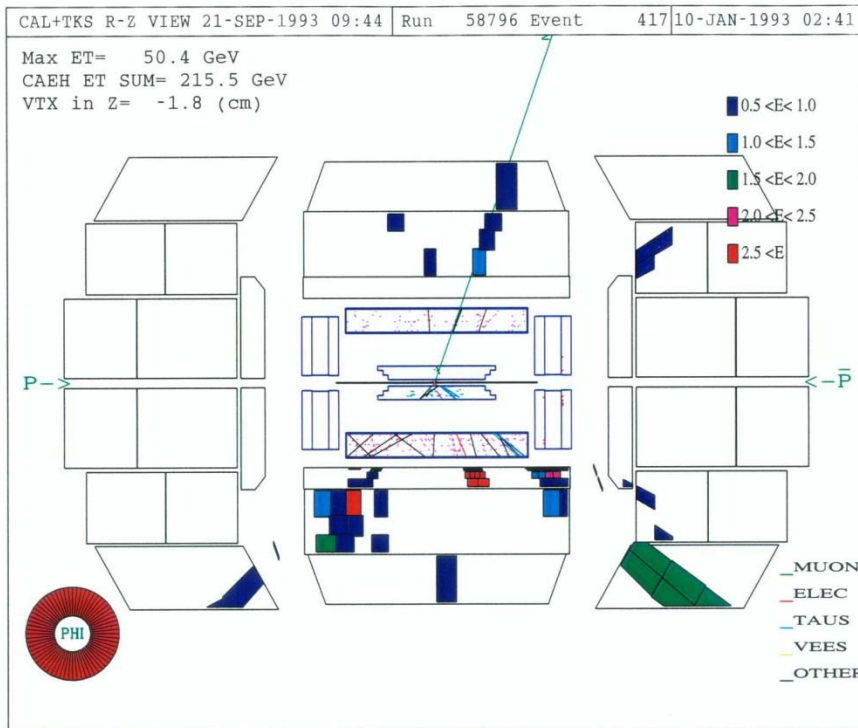


Si Tracker - 6 layers, $\sim 15\mu$ resol'n; CFT: 1 mm ϕ fibers - 8 double layers; Upgraded trigger for 6 X 6 \Rightarrow 36 X 36 bunches, new hardware and software for tracking, calorimeters & muon systems. 2T solenoid \Rightarrow p_T & q .



Top Discovery 1995

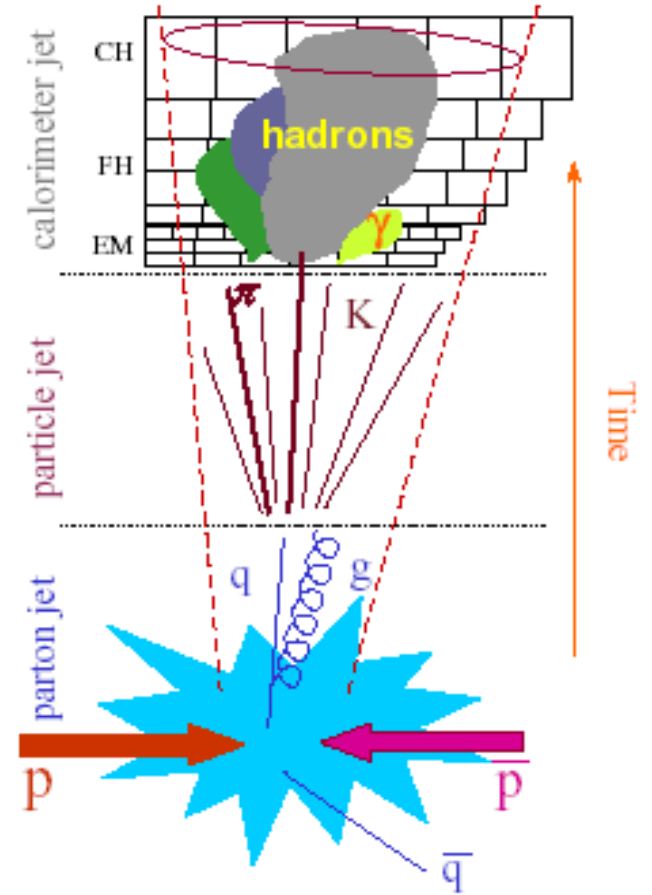
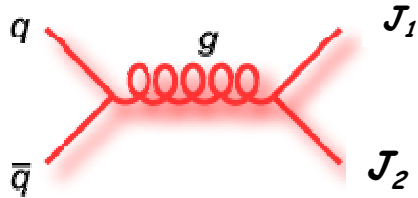
Jan 10, 1993 probable Top pair event with: $q + q' \Rightarrow t_1 + t_2$
 and $t_1 \Rightarrow W_1 + b_1, W_1 \Rightarrow e \nu$
 $t_2 \Rightarrow W_2 + b_2, W_2 \Rightarrow \mu \nu$

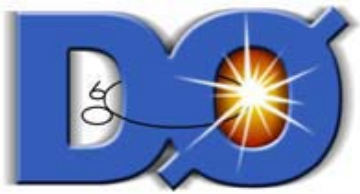




QCD

1. The Jet Energy Scale
2. The Inclusive Jet Cross Section





Jet Energy Scale in DØ

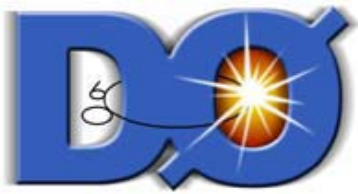
1. Use J/ψ , Upsilon, Z \Rightarrow $e^+ e^-$ to establish the EM scale, both offset due to upstream dead material and slope.
2. Study prompt photon + jet events to understand the selection and energy scale. Tune response with jet simulation studies.
3. Use p_T balance in photon plus jet events for calibration.

$$E_{jet}^{corr} = \frac{E_{jet}^{uncorr} - Off}{Show \times Resp}$$

Off = offset corrections due to noise, pile-up, ... Determined from zero-bias data.

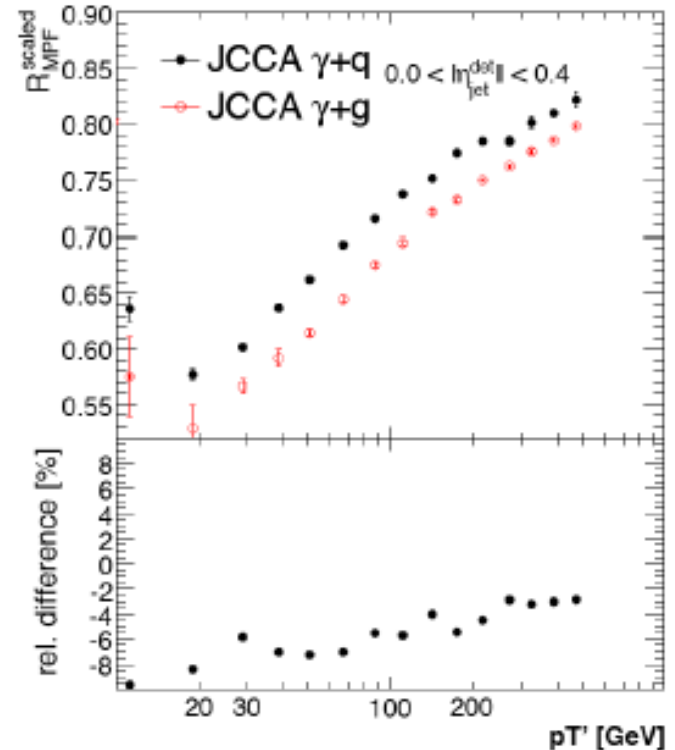
Show = showering outside 0.7 cone, dead material, etc. No corr. for physics outside of cone, $q - g$, ..

Resp = jet response – η dependent corrections; response obtained from $\gamma + jet$ events; checked with Z + jet events.



Quark/Gluon Response Differences

- Differences in quark and gluon jet response studied in γ + jet and jet-jet final states.
- Corrections depend on the physics processes. e.g. QCD jets are gluon dominated by gluons; top pair production at the Tevatron is quark dominated.

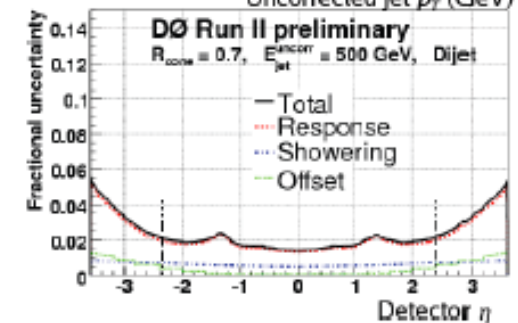
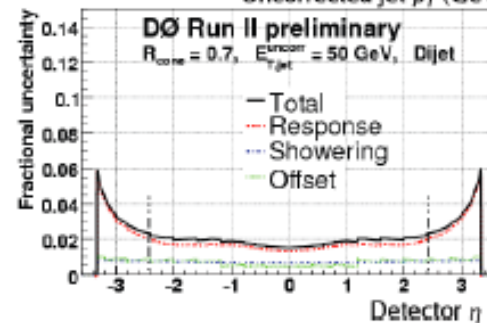
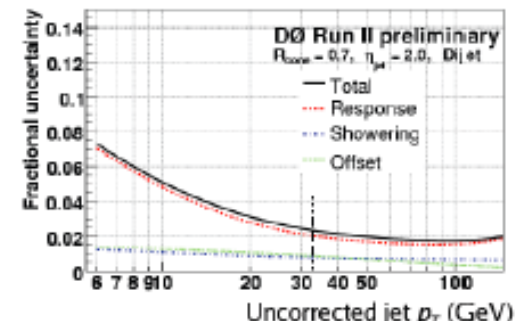


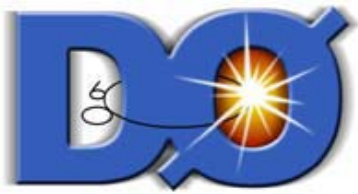


DØ Jet Energy Scale

The standard JES is determined from γ +jet balancing, but also di-jet balance is also obtained.

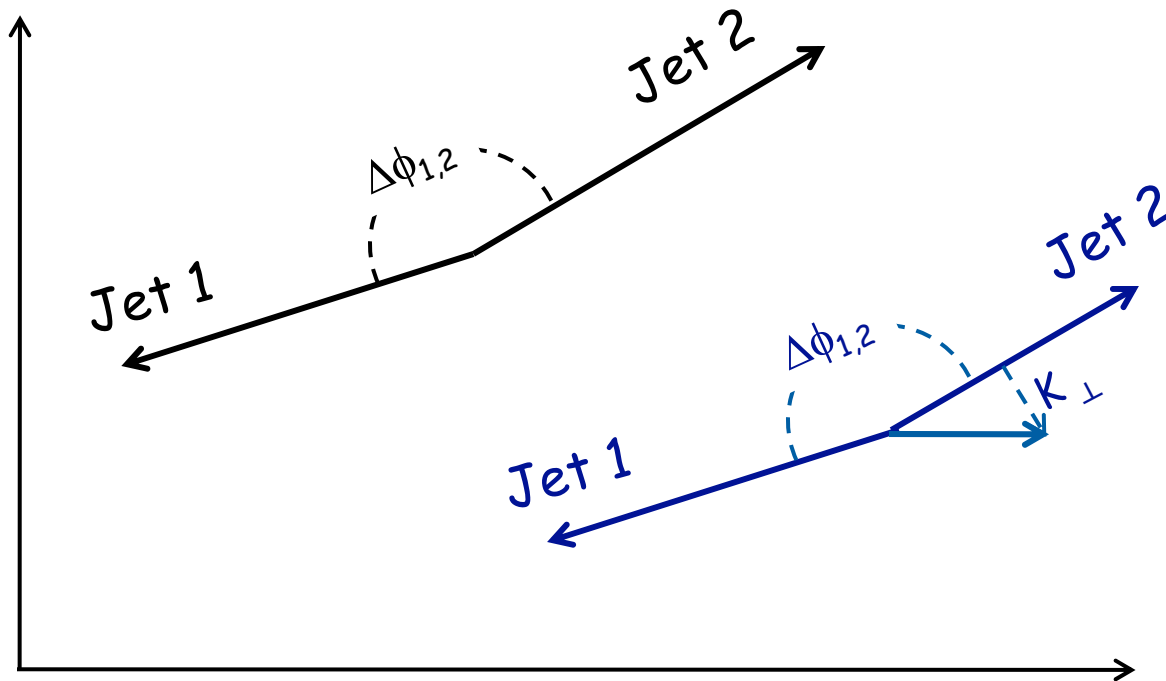
The curves shown are the response, showering, and offset corrections applied to the uncorrected jets as a function of uncorrected p_T and detector η .

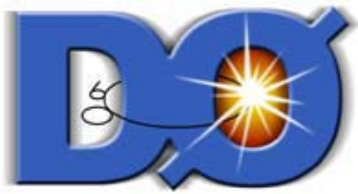




Test NLO QCD with Multi-jets

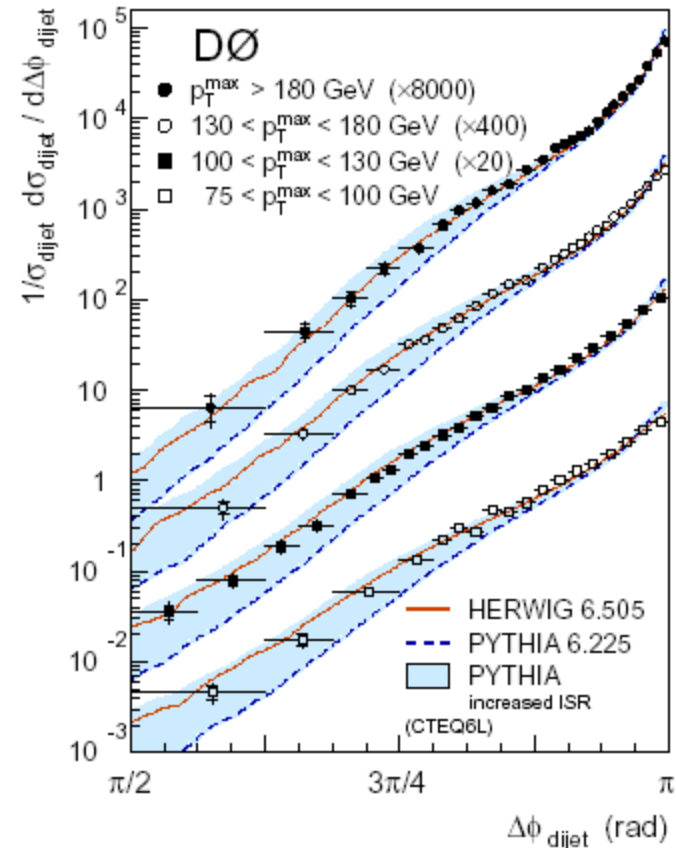
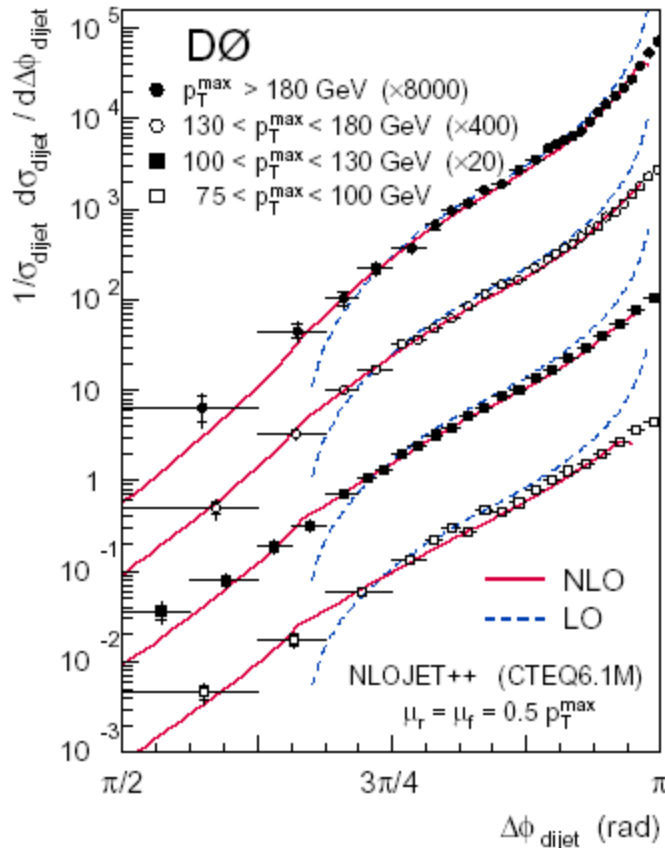
- Test of QCD multi-jets is useful exercise in preparation for measurement of: $W + \text{jets}$, $t\text{-}\bar{t}$ cross section, search for Higgs, etc.
- Measurement of the azimuthal angle between leading jets does not require a precise determination of the jet energy although we have one.





NLO QCD vs. DØ Di-jets

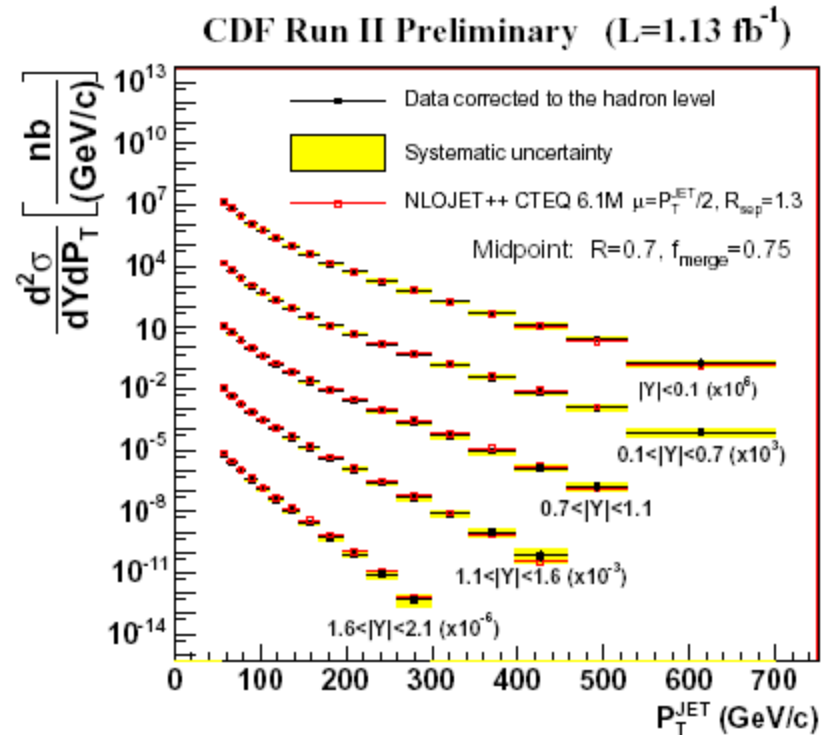
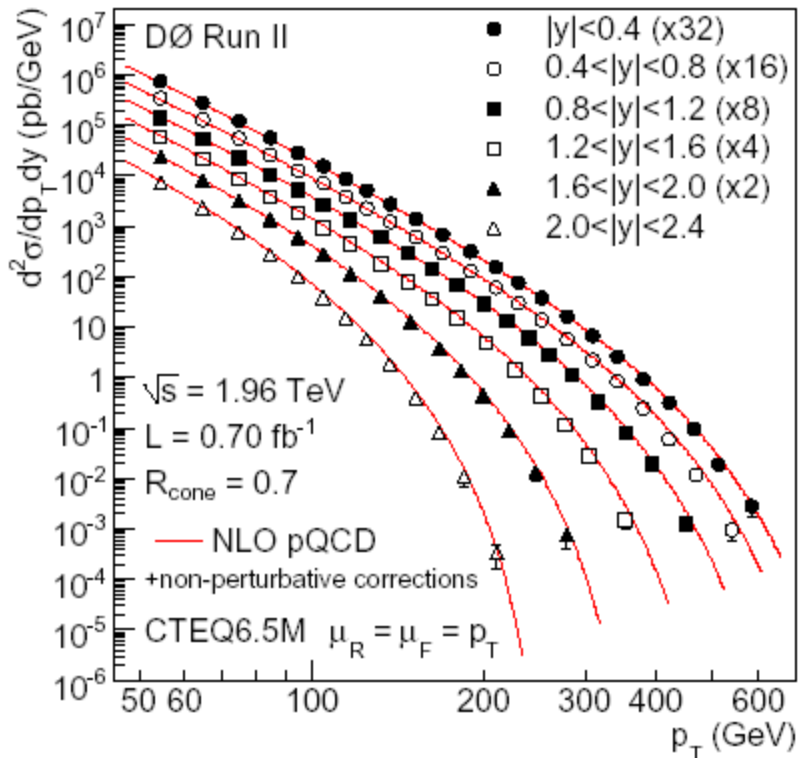
- Measure the azimuthal difference between leading jets in an inclusive QCD sample.
- NLO calculations are in good agreement with DØ data except near $\Delta\phi \Rightarrow \pi$. (soft.rad.)
- With variations in parameters both HERWIG and PYTHIA can fit the data.
- HERWIG shows a good fit at high $\Delta\phi$; PYTHIA requires add'l initial state gluon rad.

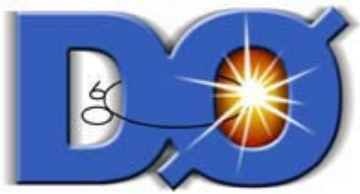




Inclusive jet cross sections: DØ & CDF

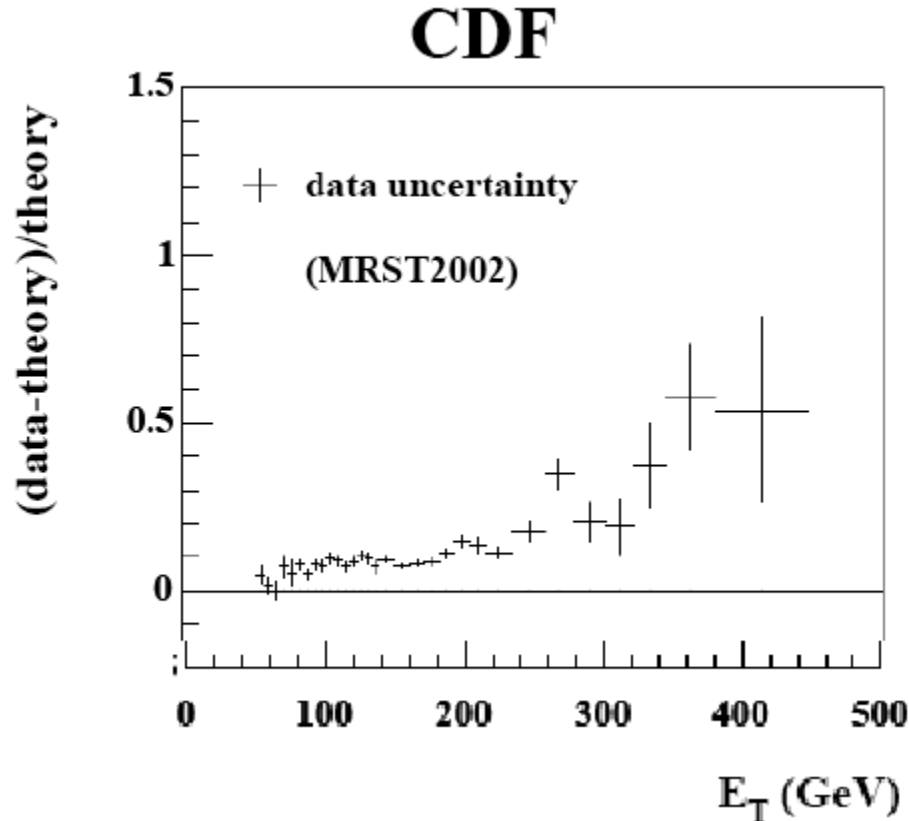
- Inclusive jet cross section for 0.7 cone algorithm: $50 < p_T < 700 \text{ GeV}$ in rapidity up to 2.1 (CDF), 2.4 (DØ). Corrections at the hadron level for DØ, the parton level for CDF.
- Comparison w/ NLO: CTEQ6.6M DØ; CTEQ6.1 CDF; $\Rightarrow \Delta\sigma(\text{CDF}) \sim 2 * \Delta\sigma(\text{DØ})$
- **Good agreement over six orders of magnitude.**

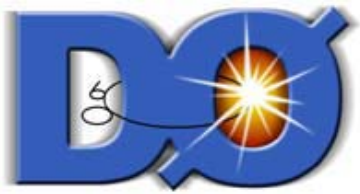




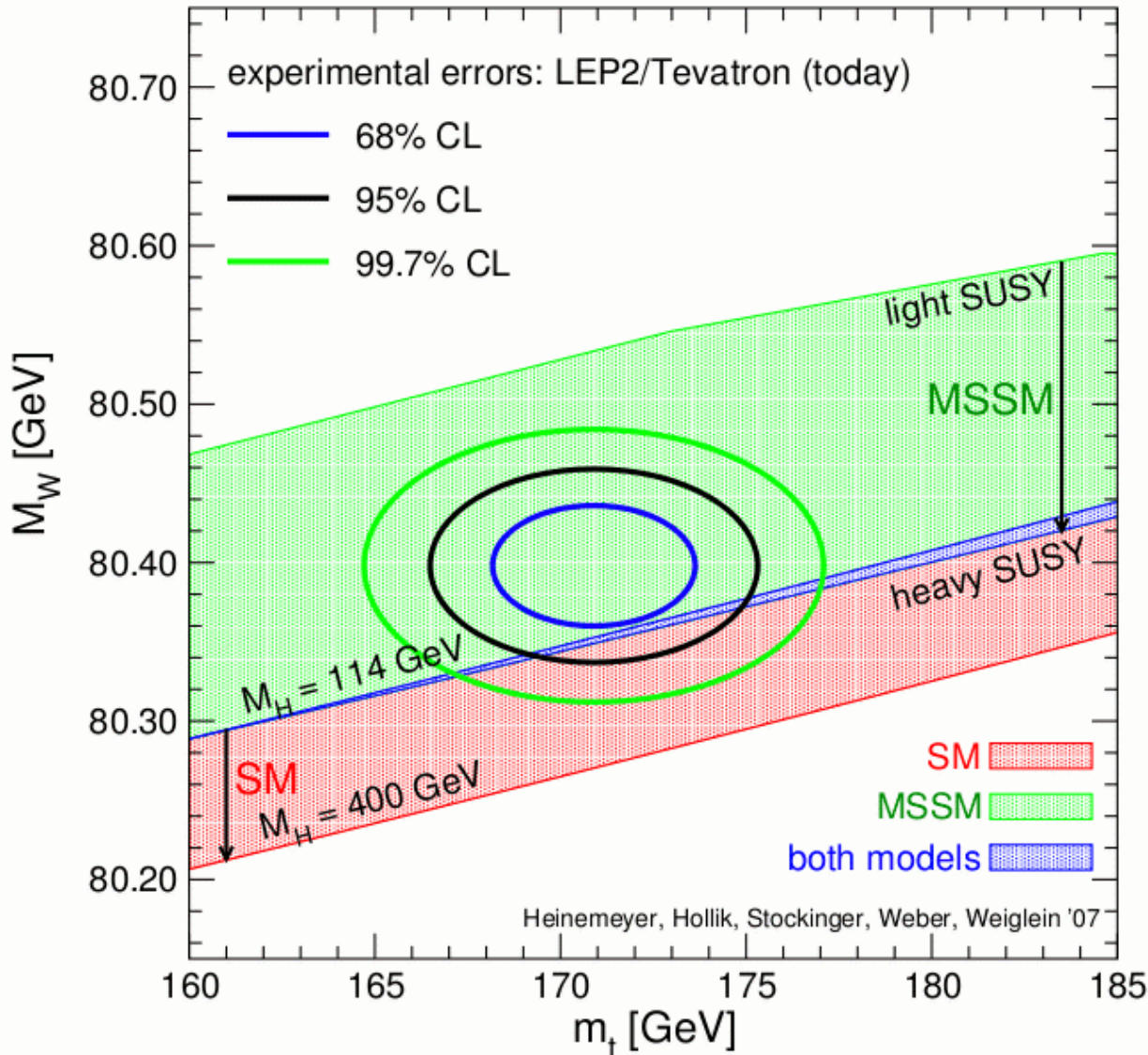
1995 CDF Excess at High E_T ?

- Initially thought it might be due to quark sub-structure or new physics.
- Now thought to be accommodated with increased gluon density at high- x .
- LHC? Will similar comparisons arise?

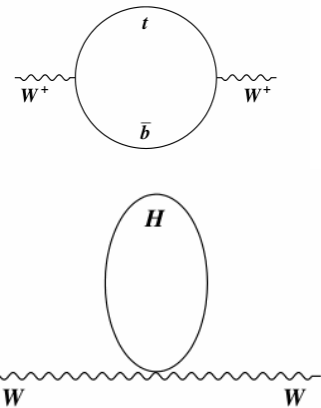




W Mass Measurement - 1fb^{-1}



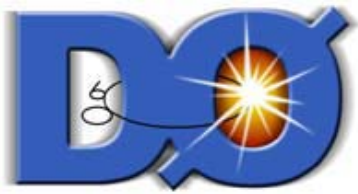
$$M_W = \sqrt{\frac{\pi\alpha}{\sqrt{2}G_F \sin\theta_W}} \frac{1}{\sqrt{1-\Delta r}}$$



$$\Delta r = f(M_t^2, \log M_H)$$

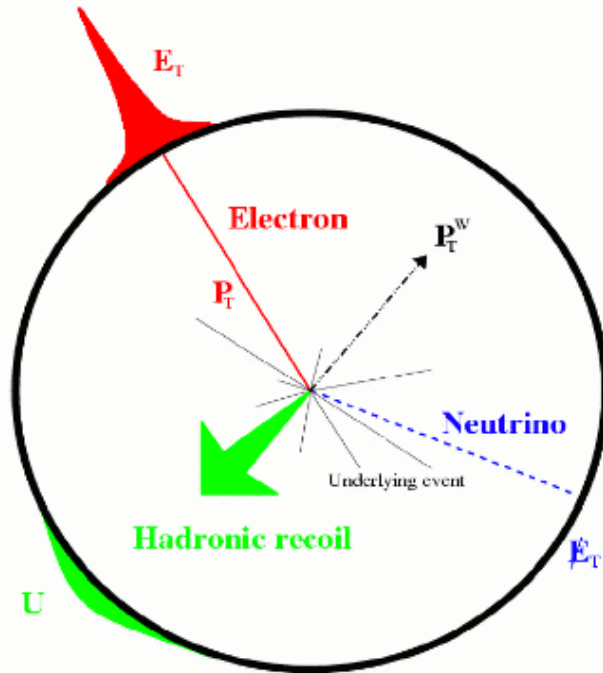
If $\Delta M_t = 1.3\text{ GeV}/c^2$, need $\Delta M_W = 8\text{ MeV}/c^2$, to make equal contributions to the Higgs mass.

2007 CDF (200pb^{-1})
 $M_W = 80413 \pm 48\text{ MeV}$
 World Avg = $80398 \pm 25\text{ MeV}$



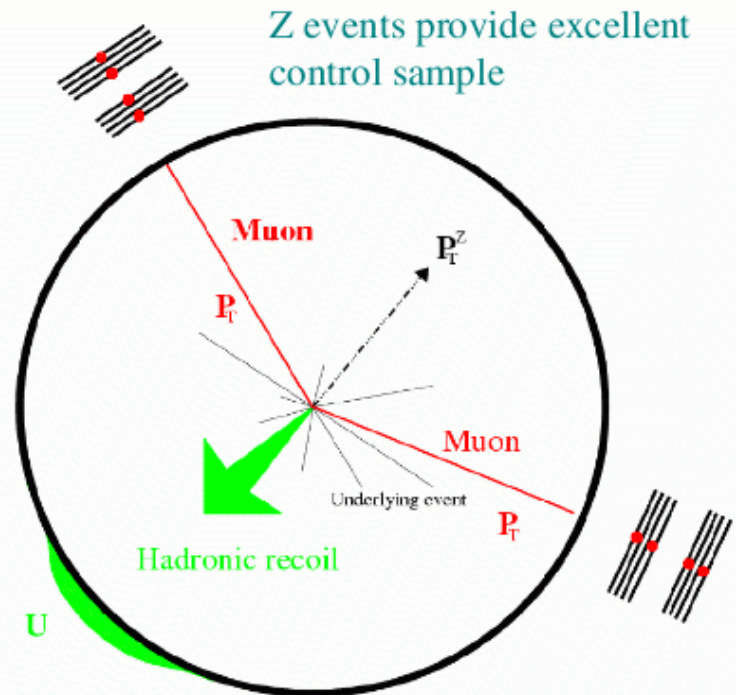
Event Sample Characteristics

1 fb⁻¹ of data; 449,830 W ⇒ e ν; 19,000 Z ⇒ e⁺ e⁻; η_e < 1.05



Typically small hadronic (jet) activity

Isolated, high p_T leptons,
missing transverse momentum in W's

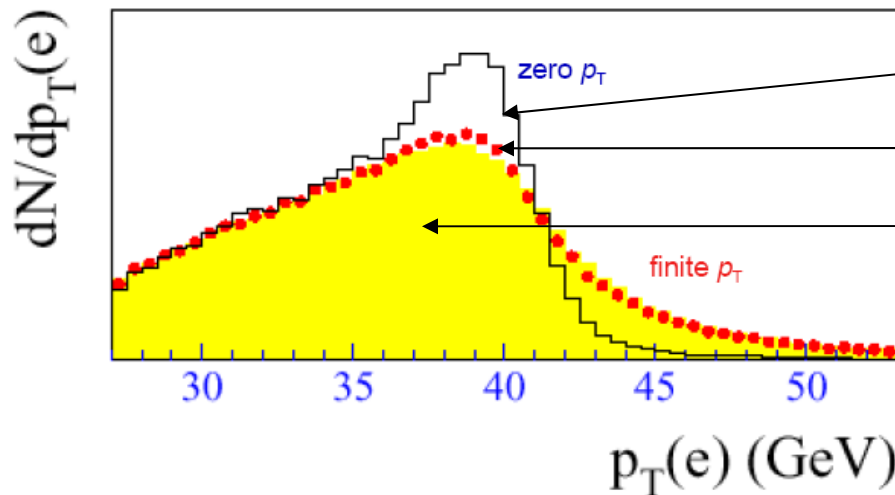


Z events provide excellent control sample

Trigger on e's plus jets. Measure one or two e's, calorimetrically, and with tracking. Measure the hadronic recoil; Reconstruct p_T(e's), p_T(jets) and infer the neutrino p_T.



Three techniques: $p_T(e)$, m_T , $p_T(\nu)$



$$P_T(W) = 0$$

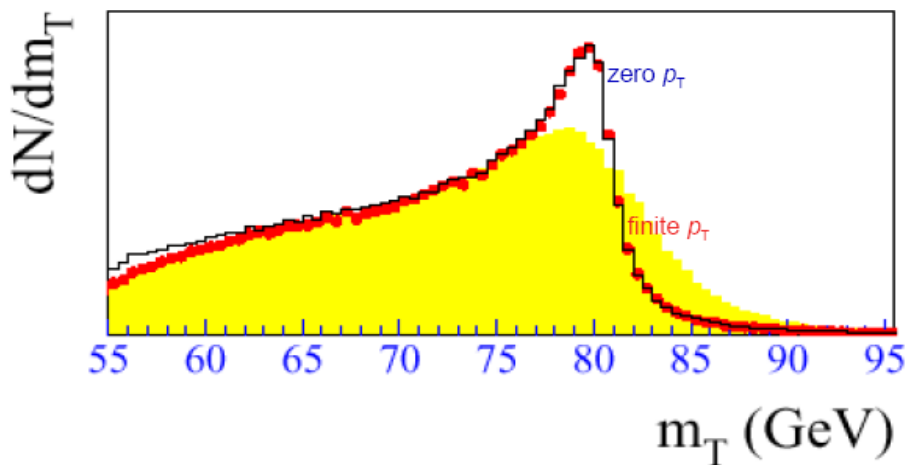
$P_T(W)$ inferred from P_T of Z's

$P_T(e)$ with detector effects

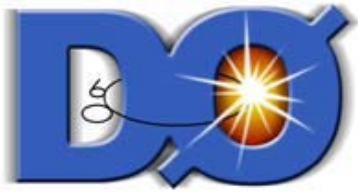
$P_T(e)$ most affected by $P_T(W)$.

$$M_T = \sqrt{2E_T^l \cancel{E}_T (1 - \cos \Delta\phi)}$$

M_T most affected by measurement of missing transverse momentum.

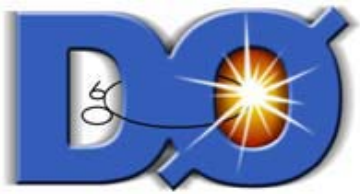


Use MC simulation to predict the shape of these observables for a given mass and detector model: **ResBos** [Balazs, Yuan; PR D56, 5558] + **Photos** [Barbiero, Was; Comp. Phys. Com. 79, 291] for W/Z prod'n & decay, plus parameterized det. model.

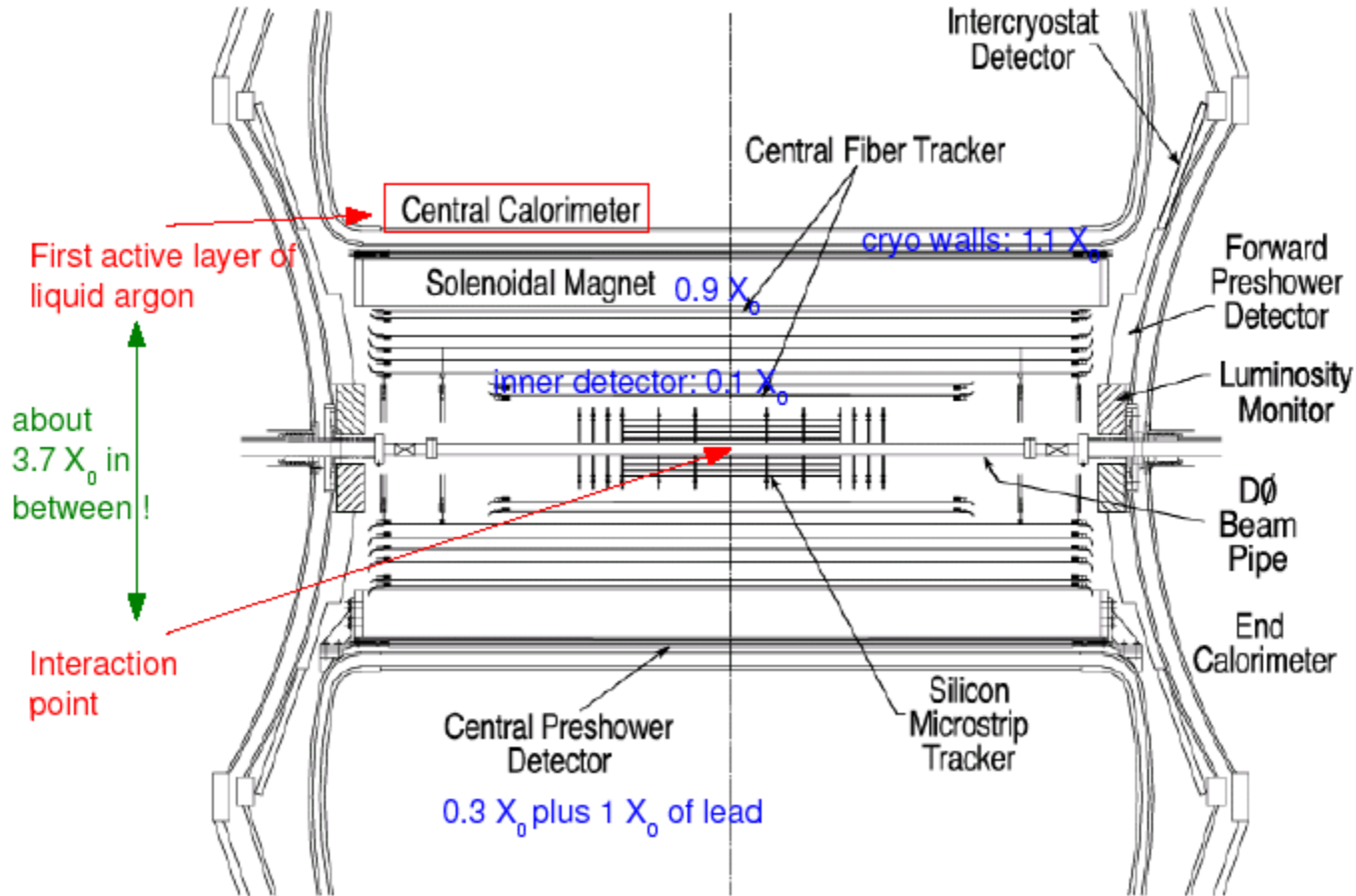


Analysis Road Map

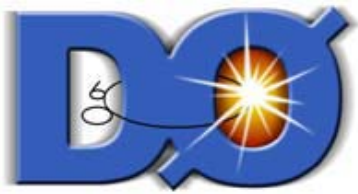
- **First: Blind MC analysis from the apparatus through analysis software.** Done to understand the full extent of detector, event generation, reconstruction, calibrations, and analysis.
- **MC event generation** - several $\times 10^8$ events. Need both $Z \Rightarrow e^+ e^-$ and $W \Rightarrow e \nu$. Developed a fast Parameterized Monte Carlo Simulation: **PMCS**.
- **W p_T distribution:** apply low p_T gluon resummation non-perturbative form factor described by $g_1, g_2 (0.68 \pm 0.02)$, and g_3 for low p_T W & Z production at the Tevatron. Use **Rebos** and **Photos** simulations for ISR/FSR. For parton distribution functions **CTEQ6.1M** and variations have been used in the generation study of event samples and systematic errors.
- **Event selection and efficiency calculations.**
- **Measure and study backgrounds:** $Z \Rightarrow e e$ w/1 e missing; jet faking an electron; underlying event effects; more than 1 collision/Xing. $\langle L \rangle (1\text{fb}^{-1}) = 41\text{E}30 \Rightarrow 1.2 \text{ events/Xing}$. Overlay min-bias and zero-bias events.
- **Electron energy response simulation.**
- **Recoil Response simulation.**



Calor. electron energy response issues



Must include dead X_0 material and its location in the E_{cal} measurement



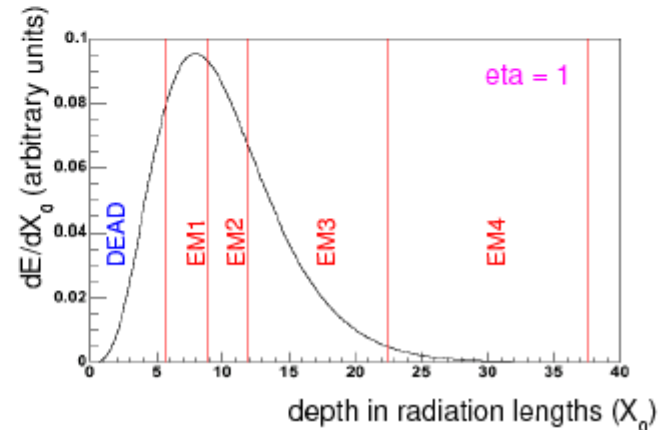
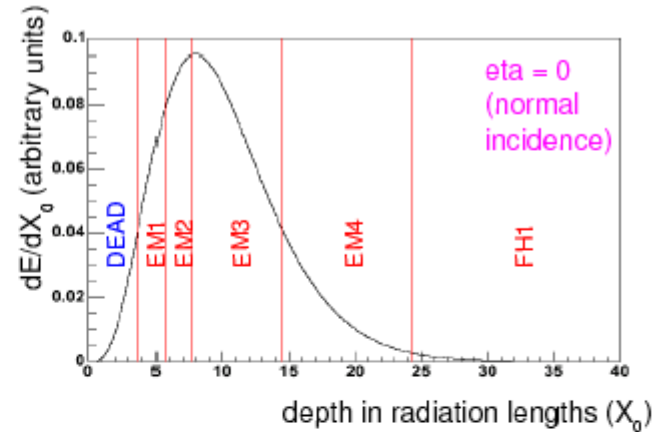
Calor. electron energy sample/weights

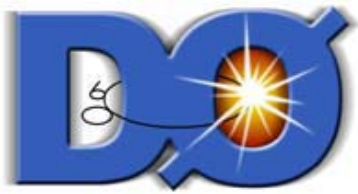
The plot on the right shows the average longitudinal profile of a shower with $E = 45$ GeV. Assuming normal incidence, the position of the active parts of the CC are also indicated.

In the reconstruction, we apply artificially high weights to the early layers (especially EM1) in an attempt to partially compensate the losses in the dead material:

Layer	depth (X_0)	weight (a.u.)	weight/ X_0
EM1	2.0	31.199	15.6
EM2	2.0	9.399	4.7
EM3	6.8	25.716	3.8
EM4	9.1	28.033	3.1
FH1	≈ 40	24.885	≈ 0.6

The lower plot illustrates the situation for the same average shower, but this time under a more extreme angle of incidence (physics $\eta = 1$). The shower maximum is now in EM1 !

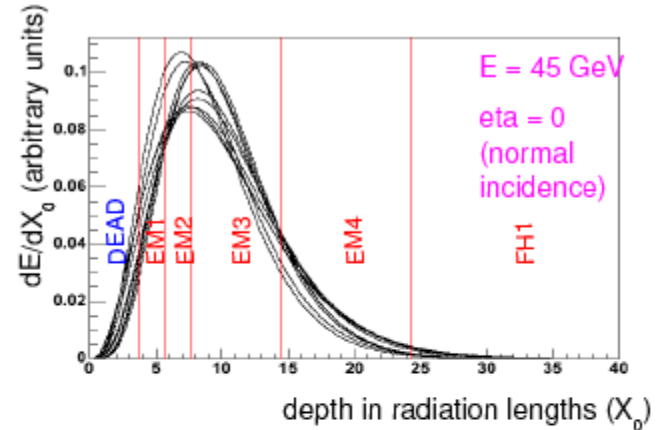




e^\pm shower energy dependence

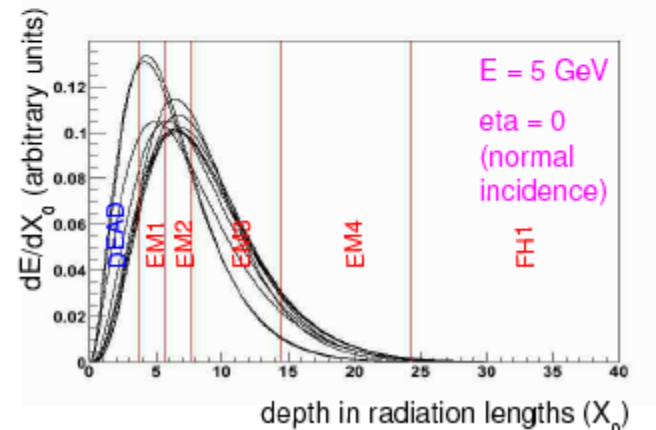
The plots on the previous slide show the *average* shower profile at $E = 45$ GeV.
The plot on the right is basically the same, except that it includes typical *shower fluctuations*.

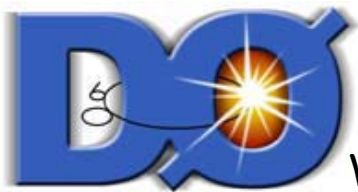
=> The fraction of energy lost in the dead material varies from shower to shower.



The bottom plot illustrates the situation at a different, lower, energy. The position of the shower maximum (in terms of X_0) varies approximately like $\ln(E)$.

=> The average fraction of energy lost in dead material, as well as the relative importance of shower-by-shower fluctuations depend on the energy of the incident electron.

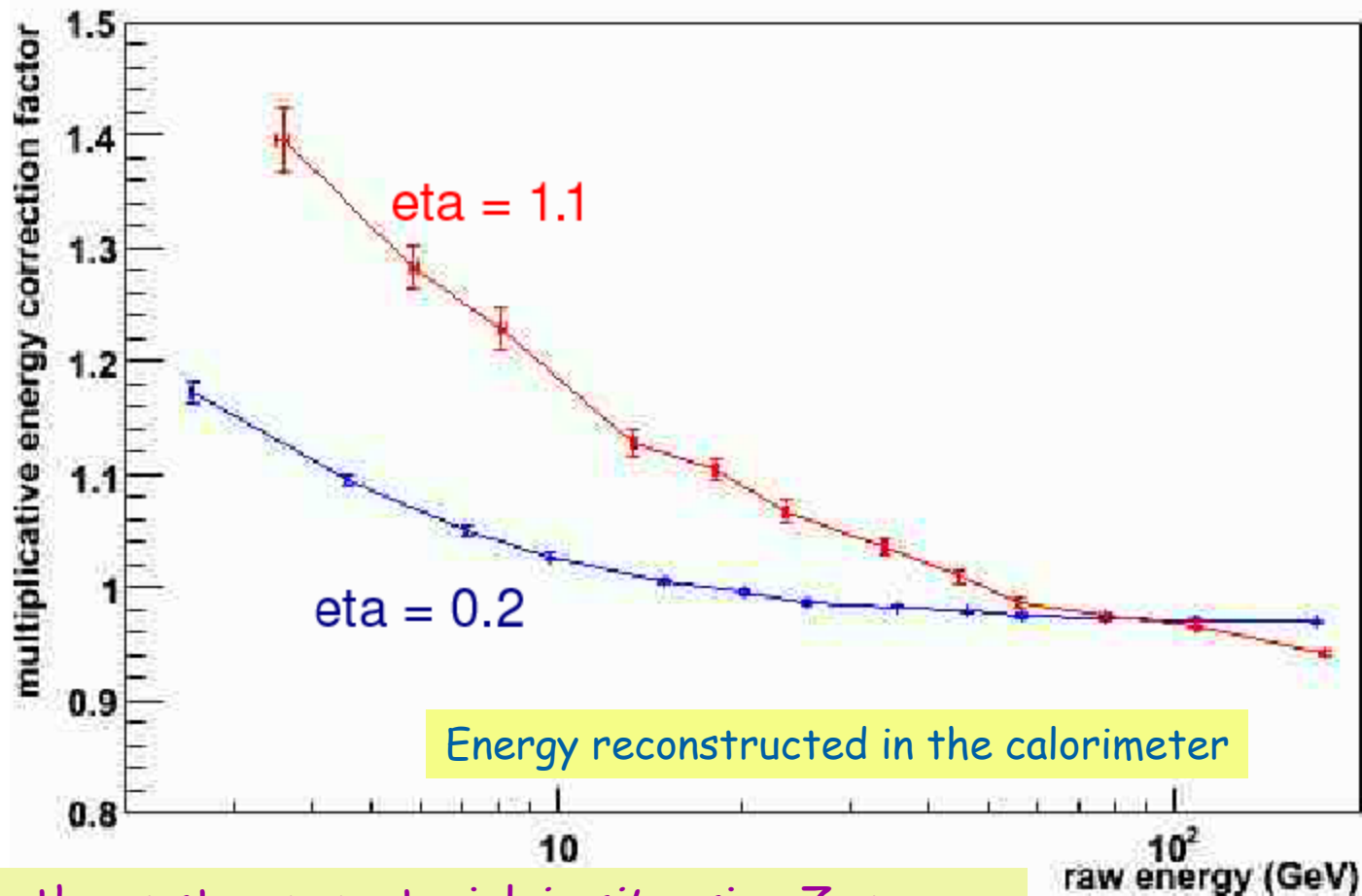




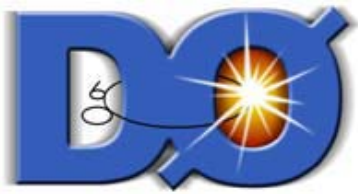
Average Response

We apply an energy loss correction to reconstructed electrons to account for the energy lost in material upstream of the calorimeters: SC coil w/cryostat, pre-shower detector, LAr cryostat walls, etc.

Factor that gets us back to the energy of the incident electron.

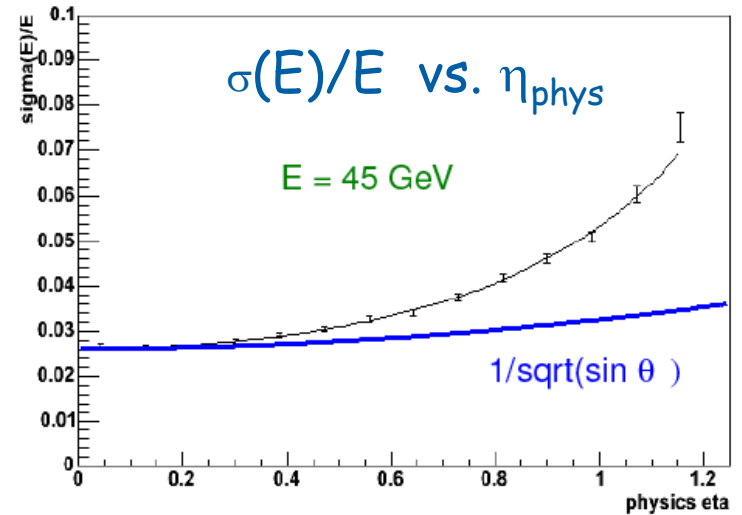
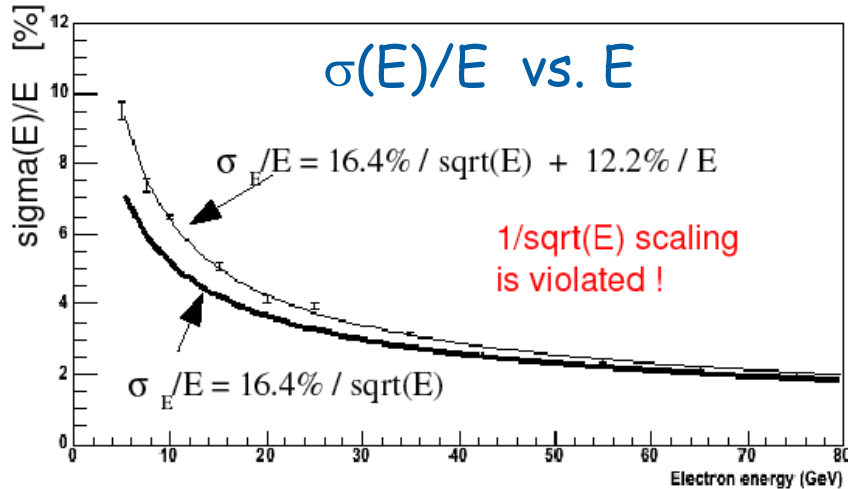


We measure the upstream material *in situ* using $Z \Rightarrow e^+ e^-$



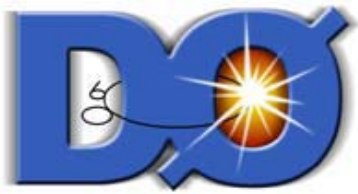
Electron Energy Resolution

Detailed simulation the D0 calor. based on GEANT simulation to determine $\sigma(E)/E$.



For a sampling calor: Expect: $\sim 1/\sqrt{E}$ \leftarrow No dead material \rightarrow $\sim 1/\sqrt{\sin \theta}$

Use the $Z \rightarrow e^+ e^-$ sample with different energy electrons to verify the dead material components.



Splitting the $Z \Rightarrow e e$ Sample

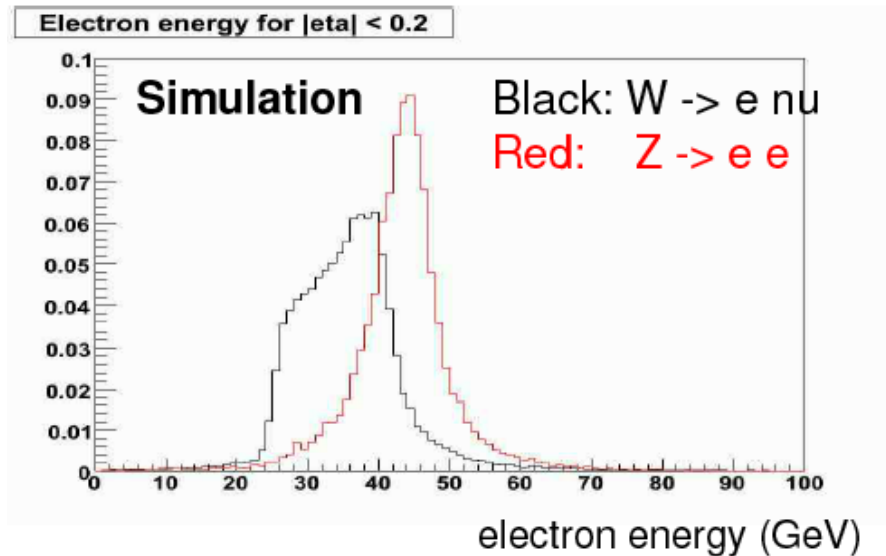
$Z \Rightarrow e^+ e^-$ gives the kinematic connection to energy and angle space for the CC.

Proceed by:

- \Rightarrow Bin electrons in angle (5 η -bins).
- \Rightarrow 2 e's per Z.
- \Rightarrow 15 allowed combinations; no energy ordering.

Split the CC/CC $Z \Rightarrow e^+ e^-$ into the 15 categories to study the measured M_Z and $\sigma(M_Z)$.
 (mass) (resolution)

Since the Z has higher mass than the W, we must propagate this information to lower electron energies.



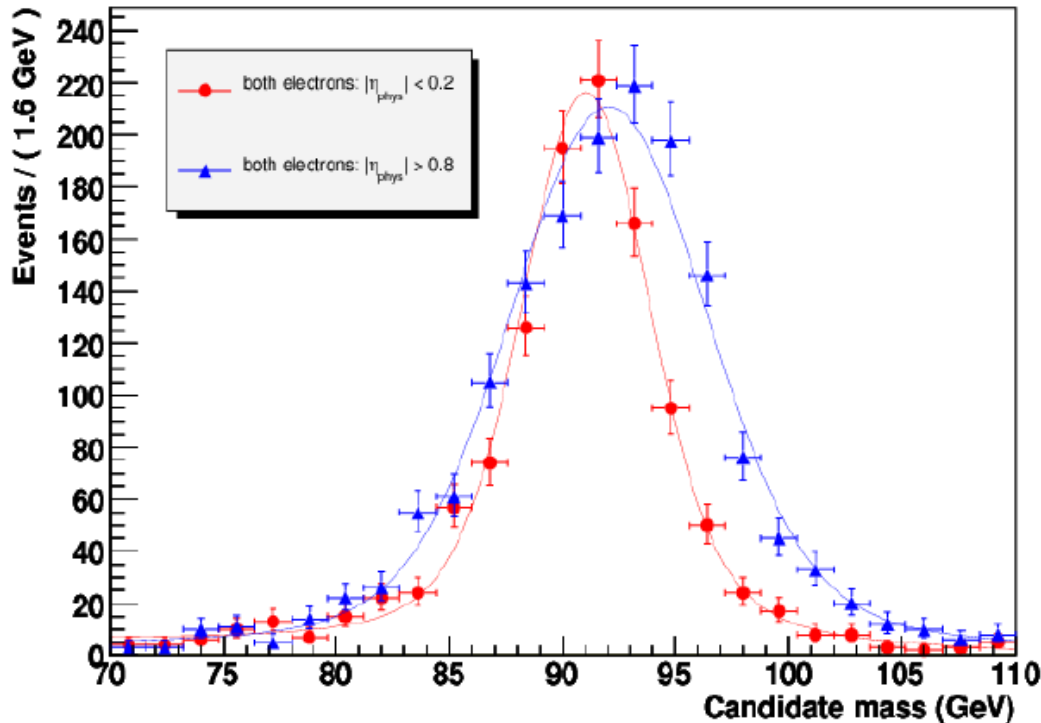
bin 0 : $0 \leq \eta < 0.2$
bin 1 : $0.2 \leq \eta < 0.4$
bin 2 : $0.4 \leq \eta < 0.6$
bin 3 : $0.6 \leq \eta < 0.8$
bin 4 : $0.8 \leq \eta $

Category	Bins of Each Electron
10	0-0
11	0-1
12	0-2
13	0-3
14	0-4
15	1-1
16	1-2
17	1-3
18	1-4
19	2-2
20	2-3
21	2-4
22	3-3
23	3-4
24	4-4



A Plot from Z Split Samples

$Z \rightarrow e e$ (both electrons in Central Cryostat)



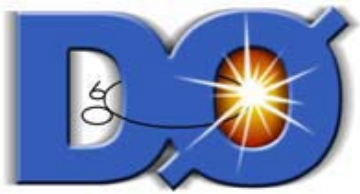
Z mass peaks for two η regions do not agree (early version of data reconstruction):

$|\eta_{\text{phys}}| < 0.2$ central (e^+, e^-)
 $e^+ e^-$ near normal incidence.

$|\eta_{\text{phys}}| > 0.8$ forward (e^+, e^-)
 $e^+ e^-$ highly non-normal incidence.

Different resolutions; different energy loss; calibration problem?

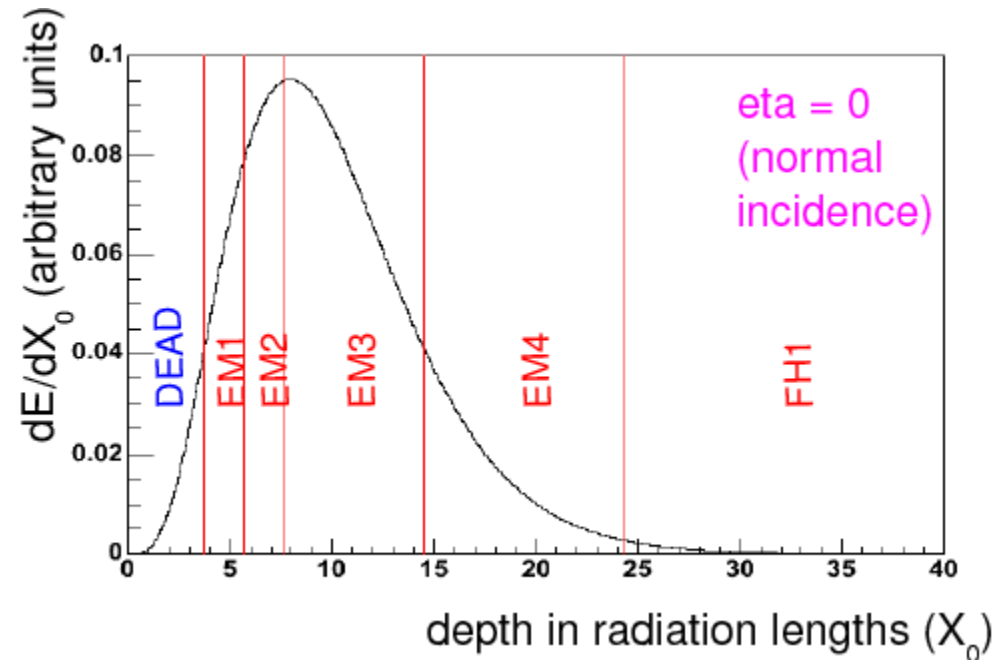
Various possibilities for the difference; additional information is needed.



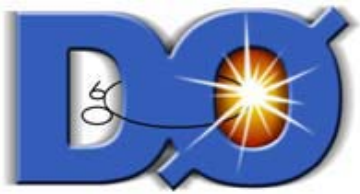
Additional Observables

Go back to one of the plots presented earlier where we noted that the longitudinal segmentation of the EM CAL provided a way to estimate the un-instrumented material in each segment.

If the depth of the dead region is extended then the various layers, EM1 through FH1 would sample different regions of the shower and thus see different fractions of the shower energy.

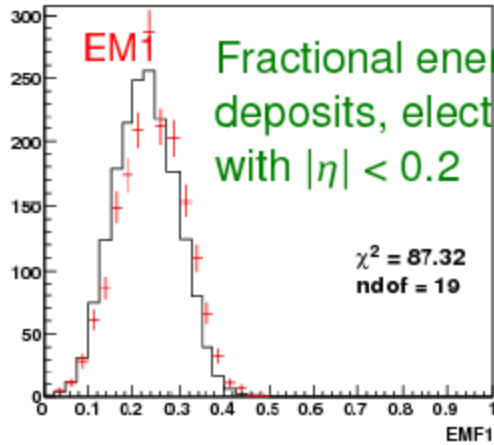


Go back to the 15 η split Z sample combinations and study the four depth layers of the EM calorimetry in each to see if a consistent picture can be made.

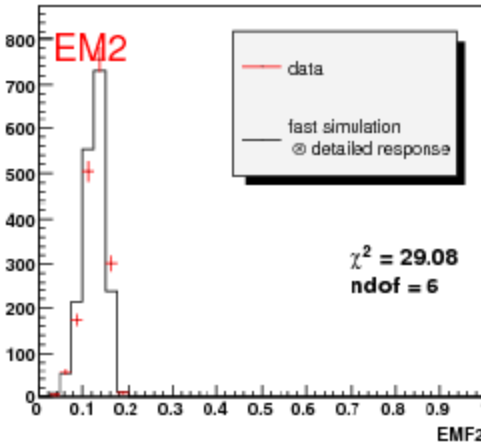


Checks on EM Layers (before)

TOYEemf_1_10



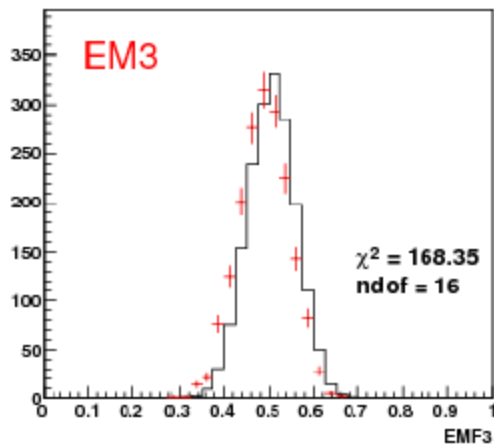
TOYEemf_2_10



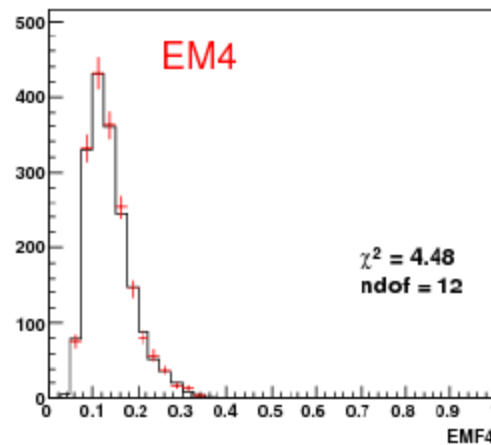
$$|\eta| < 0.2$$

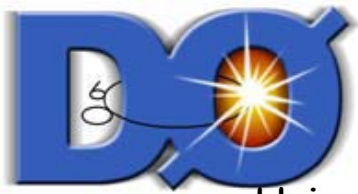
Before making any adjustments in dead material the fractional energy deposits in simulation and data do not match very well, as evidenced by the χ^2 values.

TOYEemf_3_10



TOYEemf_4_10



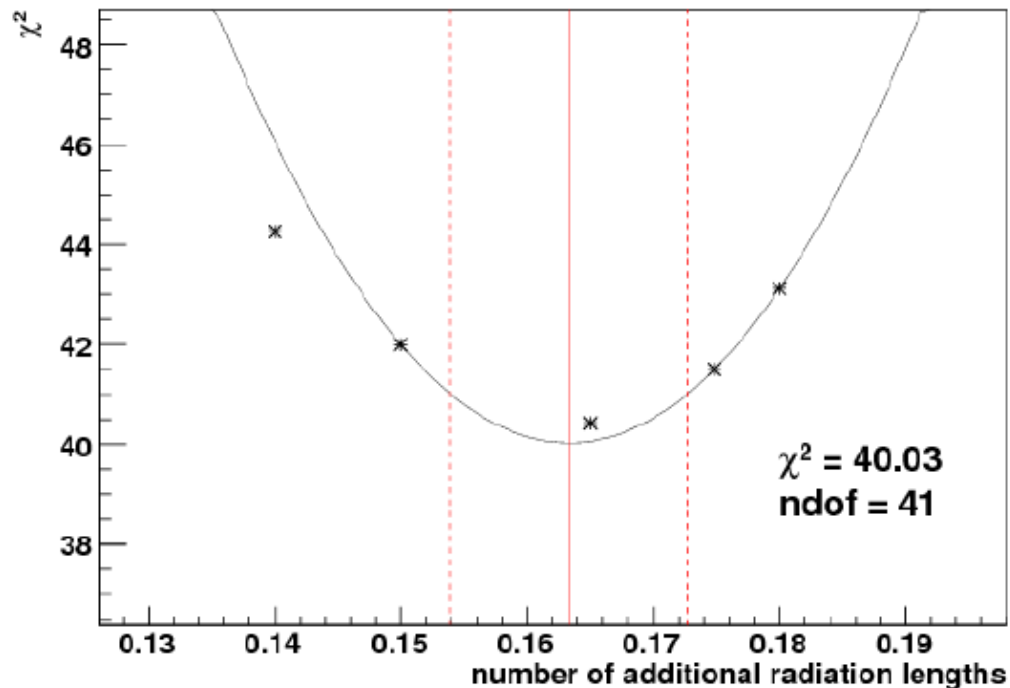


χ^2 Minimization for Extra Material

Using the data/MC ratios per η category for EM1, EM2 and EM3, fit each one separately to a constant. Add the χ^2 's from the from the EM1, EM2 and EM3 and minimize the global χ^2 from the three fits.

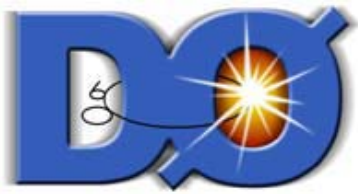
This means the absolute energy scale per layer free to float. This allows an independent inter-calibration of the EM1, EM2 and EM3 layers.

Fit for nX_0 from longitudinal shower profiles in $Z \rightarrow e e$



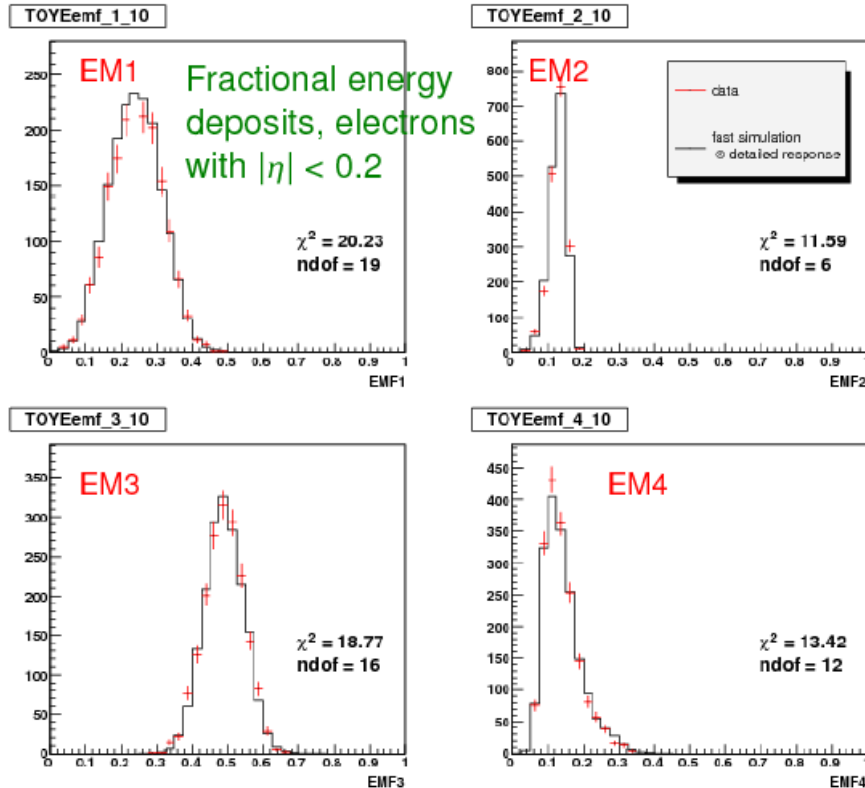
χ^2 minimization for additional nX_0 from longitudinal shower profiles.

The amount of additional material is known to $< 0.01 X_0$ with small systematics from background (underlying event) subtraction and modeling of cut efficiencies.

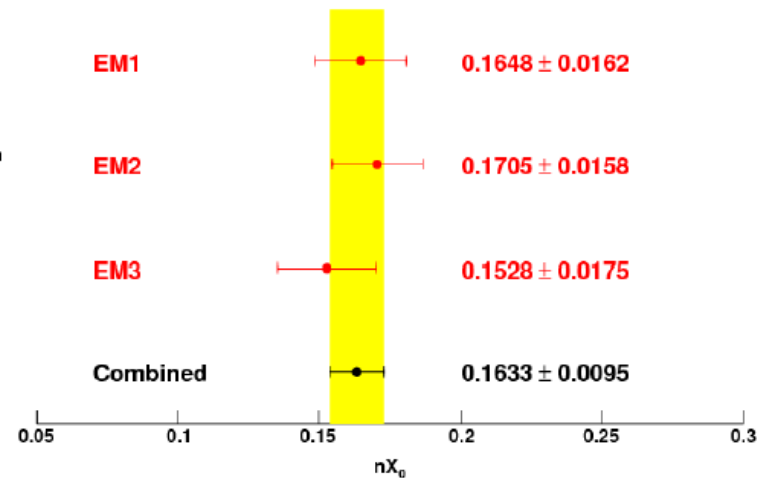


After Tuning nX_0 - Shower Profiles

After tuning the material model, distributions of fractional energy deposits agree well w/simulation.



As a cross-check the fitting to determine nX_0 has been redone separately for each EM layer. Good consistency is found.





E_e Energy Scale

After correcting for uninstrumented material the final energy response calibration is done using $Z \Rightarrow e^+ e^-$, the known Z mass from LEP (91.188 GeV), and the standard “ f_z method”.

$$E_{\text{meas}} = \alpha \times E_{\text{true}} + \beta.$$

Use the energy spread of the electrons in Z decay to constrain α and β .

$$f_z = [E(e_1) + E(e_2)]^* [1 - \cos(\gamma_{ee})] / m_Z. \quad \gamma_{ee} \text{ is the } e^+, e^- \text{ opening angle.}$$

The f_z variable allows the partitioning of the Z sample of $e^+ e^-$ decays into subsamples of different E_{true} , so that the electron energy response can be scanned as a function of α and β .

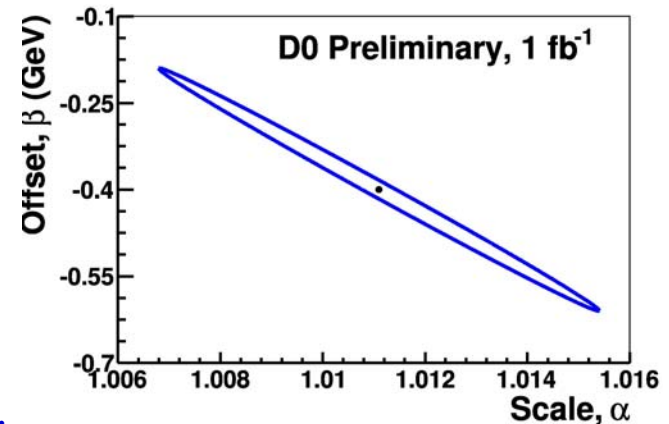
Result:

$$\alpha = 1.0111 \pm 0.0043$$
$$\beta = -0.404 \pm 0.209 \text{ GeV}$$

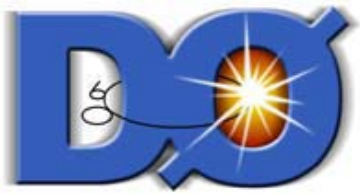
correlation: -0.997

This is the dominant systematic error for the W mass and it leads to:

$\Delta m(W) = 34 \text{ MeV}$, which is 100% correlated with $p_T(e)$, m_T , and $p_T(\nu)$ methods.



The mass resolution is driven by two components: sampling fluctuations and the constant term which is extracted from the W width meas. $C = (2.05 \pm 0.10)\%$.



Recoil Model

Recoil vector in parameterized MC :

$$\vec{u}_T = \vec{u}_T^{Hard} + \vec{u}_T^{Soft} + \vec{u}_T^{Elec} + \vec{u}_T^{FSR} \quad \text{where :}$$

$\vec{u}_T^{Hard} = \vec{f}(\vec{q}_T)$ Hard component that balances the vector boson in the transverse plane.

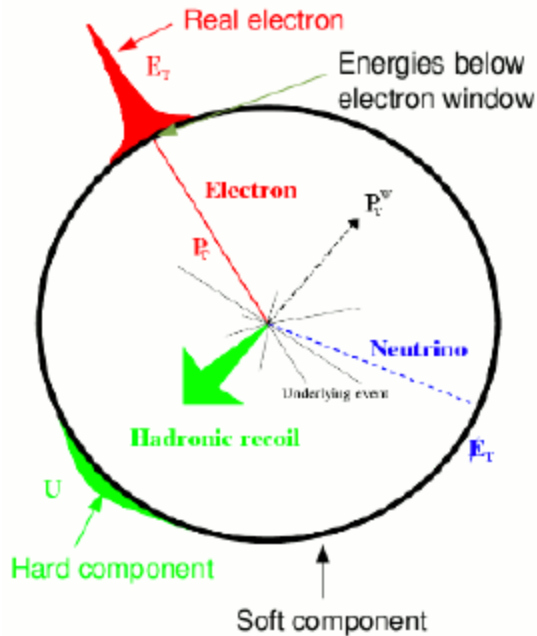
Ansatz from $Z \rightarrow \nu \bar{\nu}$ MC, jet res....

$\vec{u}_T^{Soft} = \alpha_{MB} \cdot \vec{E}_T^{MB} + \alpha_{ZB} \cdot \vec{E}_T^{ZB}$ Soft component, not correlated with vector boson. Two sub - components : add'l $p\bar{p}$ ZB evts plus spectator partons from MB evts ..

$$\vec{u}_T^{Elec} = - \sum_e \Delta u_{||} \cdot \hat{p}_T(e) \quad \text{Recoil } E \text{ lost into } e \text{ cones.}$$

$$\vec{u}_T^{FSR} = \sum_{\gamma} \vec{p}_T(\gamma) \quad \text{FSR photons (internal brems.).}$$

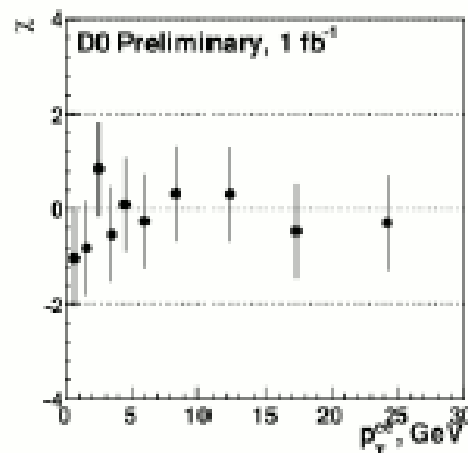
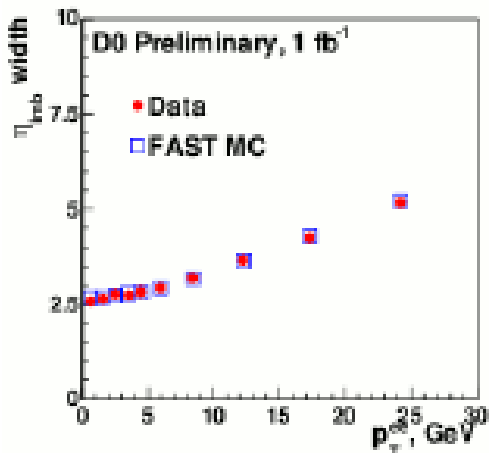
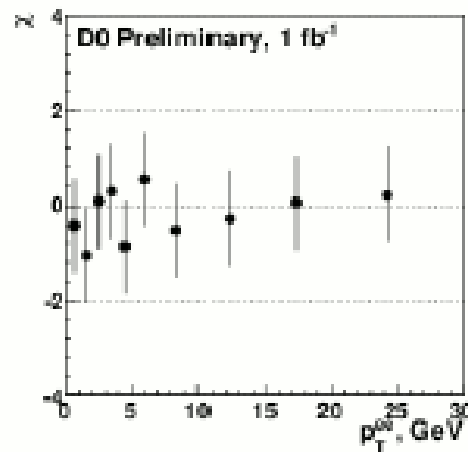
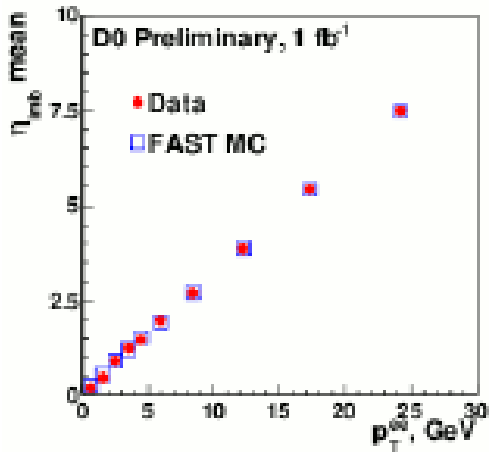
outside cone; incl. detailed resp.



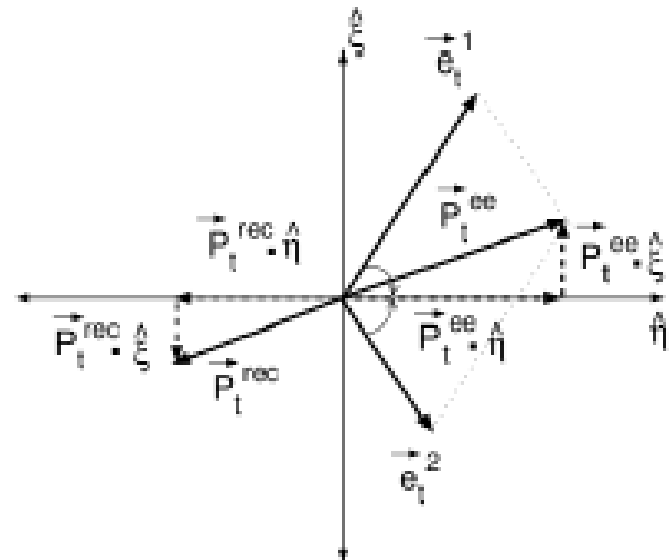


Z => e+ e- Recoil Calibration

Final adjustment of the free parameters in the recoil model is done with the Z => e e events. The sum of $p_T(\text{recoil})$ and $p_T(e+e-)$ projected on the e+ e- bisector η -axis is balanced when the measured & MC means and widths agree.



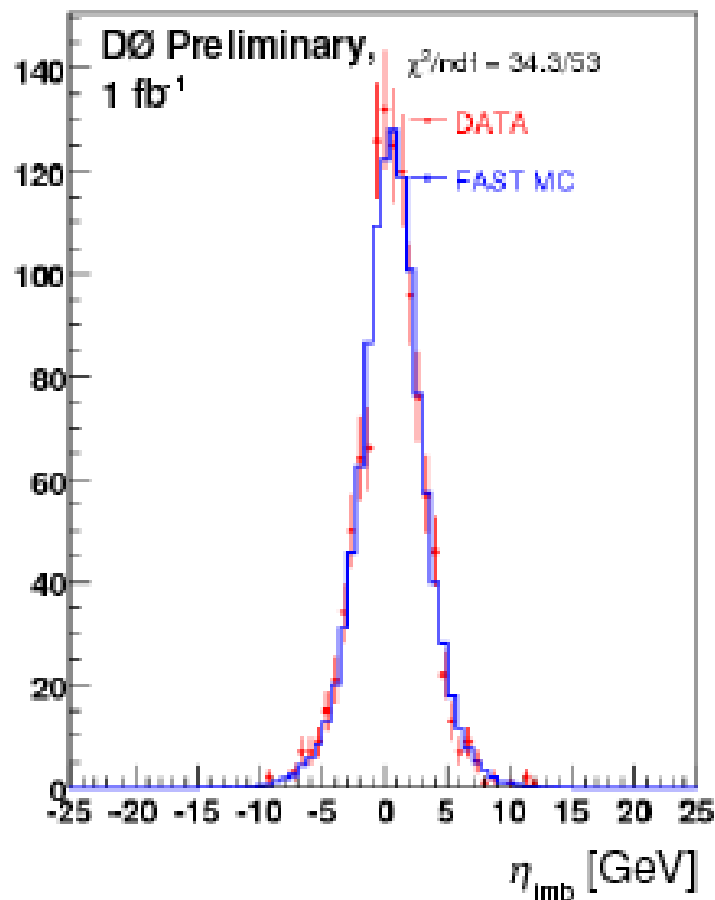
UA2 observables: In the transverse plane, use a coordinate system where the η -axis is defined by the bisector of the two electrons' momenta.



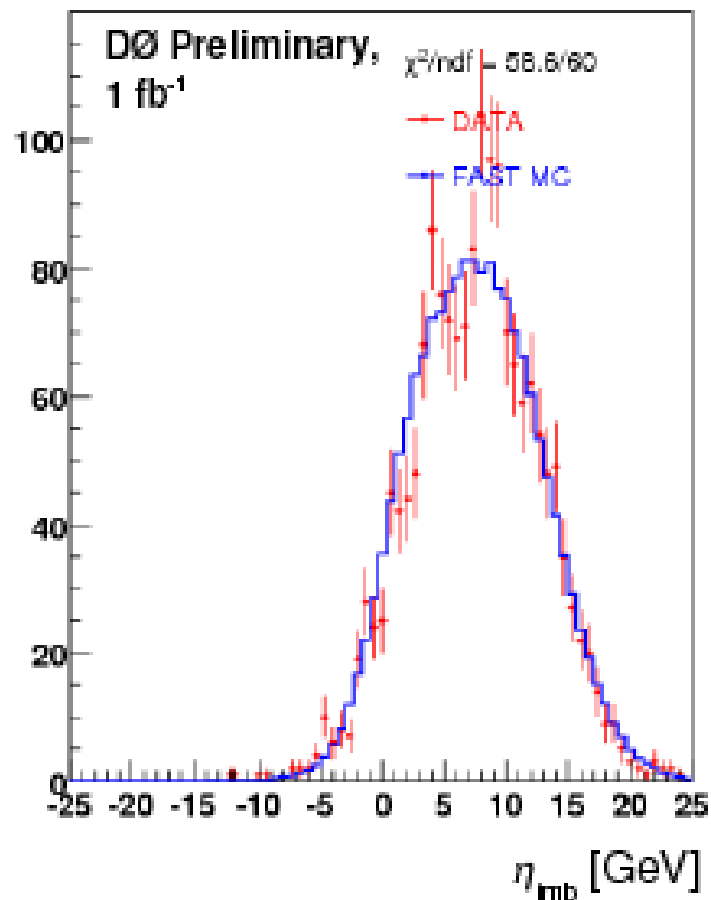


η_{imb} Example Distributions

$1 < p_T(\text{ee}) < 2 \text{ GeV}$



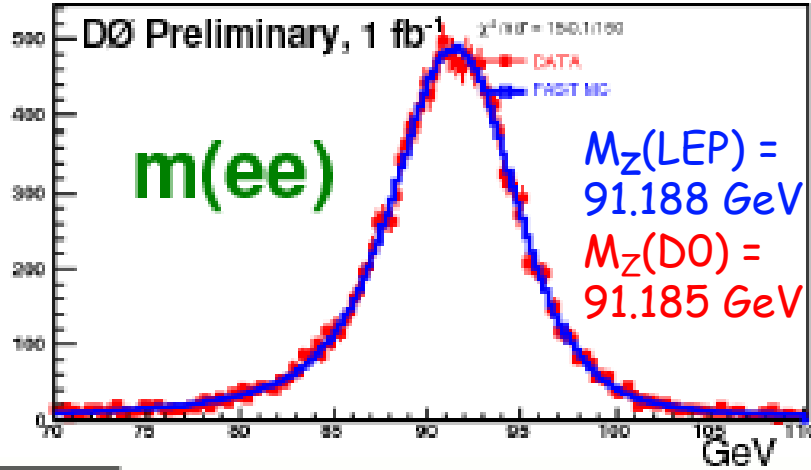
$20 \text{ GeV} < p_T(\text{ee})$



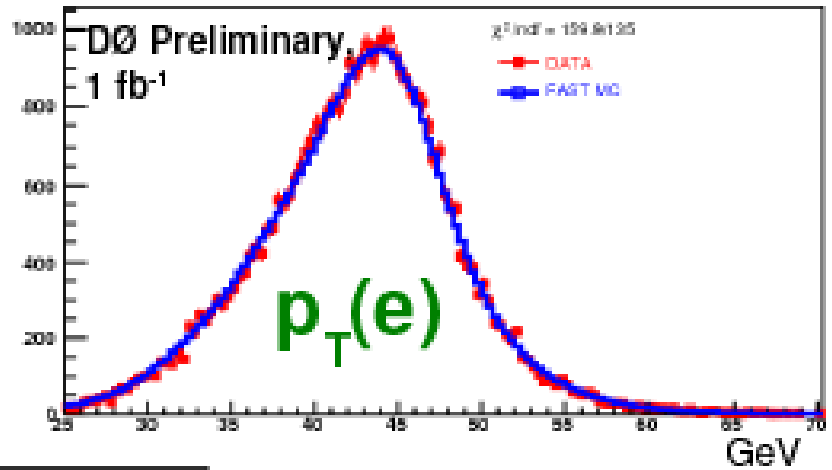


Z \Rightarrow e+ e- Results

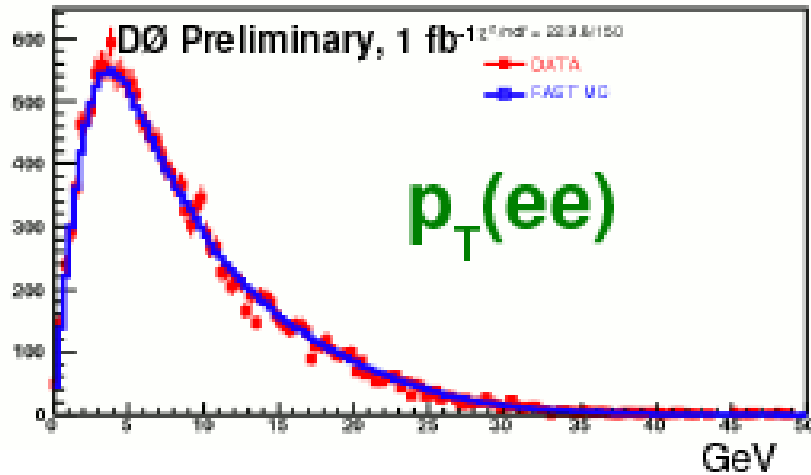
ZCandMass_C00C_Tks



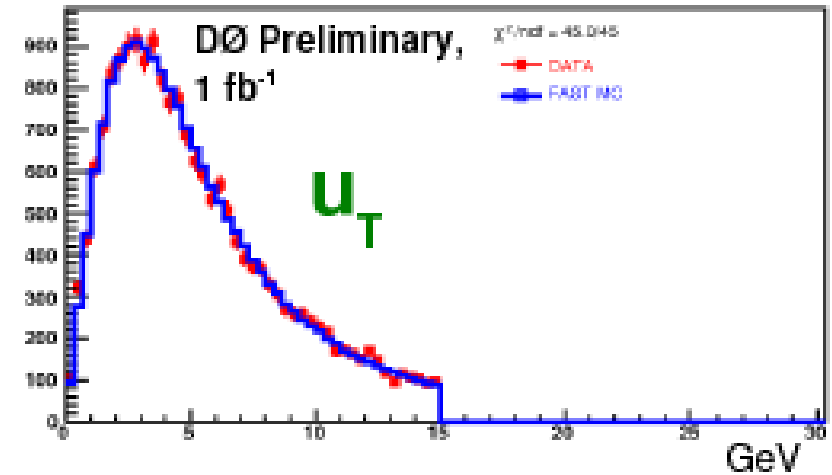
ZCandElecPt_0



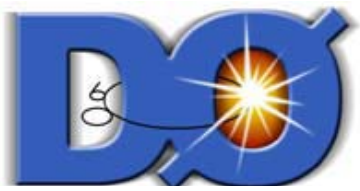
ZCandPt_0



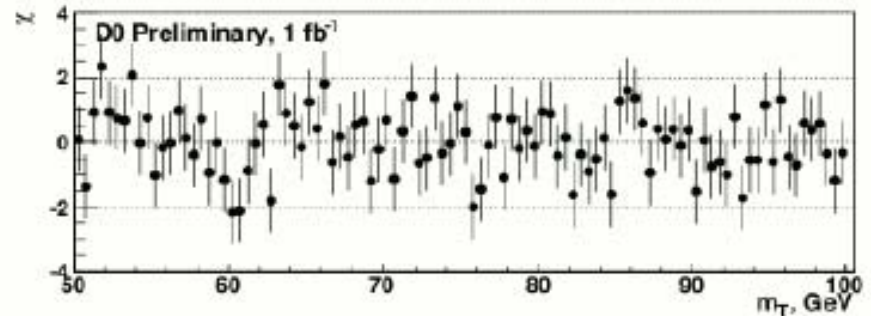
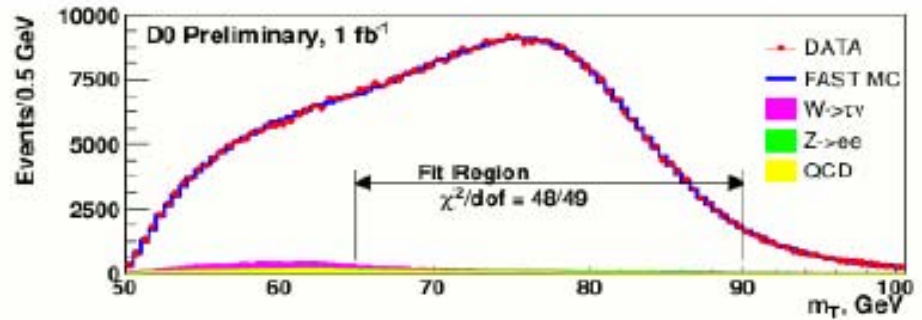
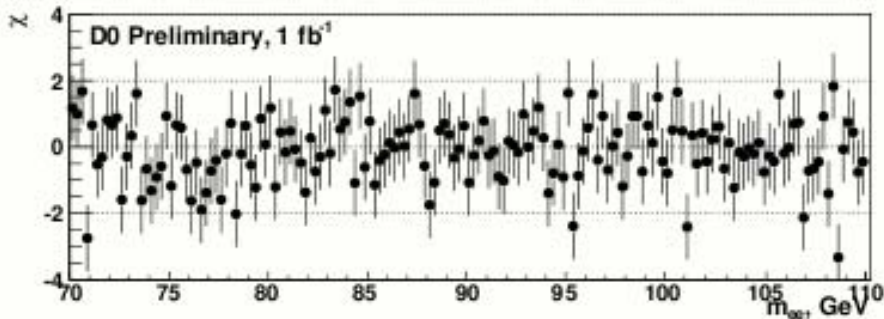
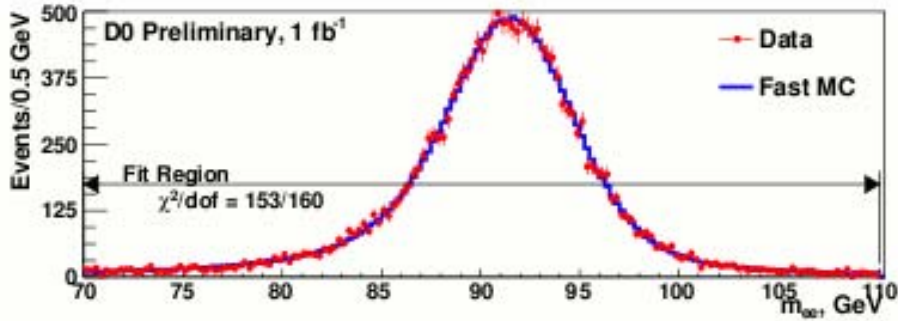
ZCandRecoilPt_0



Good agreement between parameterized MC and Z \Rightarrow e+ e- data



DØ Fitted Masses



$$M_Z = 91.185 \pm 0.033(\text{stat.}) \text{ GeV}$$

$$M_W = 80.401 \pm 0.023(\text{stat.}) \pm 0.037(\text{syst.}) \text{ GeV}$$

$$= 80.400 \pm 0.027(\text{stat.}) \pm 0.040(\text{syst.}) \text{ GeV}$$

$$= 80.402 \pm 0.023(\text{stat.}) \pm 0.044(\text{syst.}) \text{ GeV}$$

$$= 80.401 \pm 0.021(\text{stat.}) \pm 0.038(\text{syst.}) \text{ GeV}$$

Transverse Mass

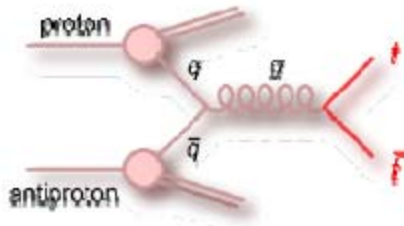
$p_T(e)$

ME_T

Average value

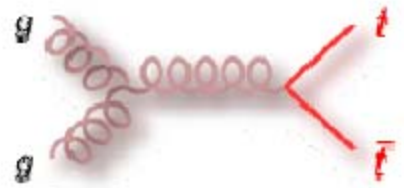


Top Quark - After 14 Years



Production is mostly via $q\text{-}\bar{q}$ annihilation.

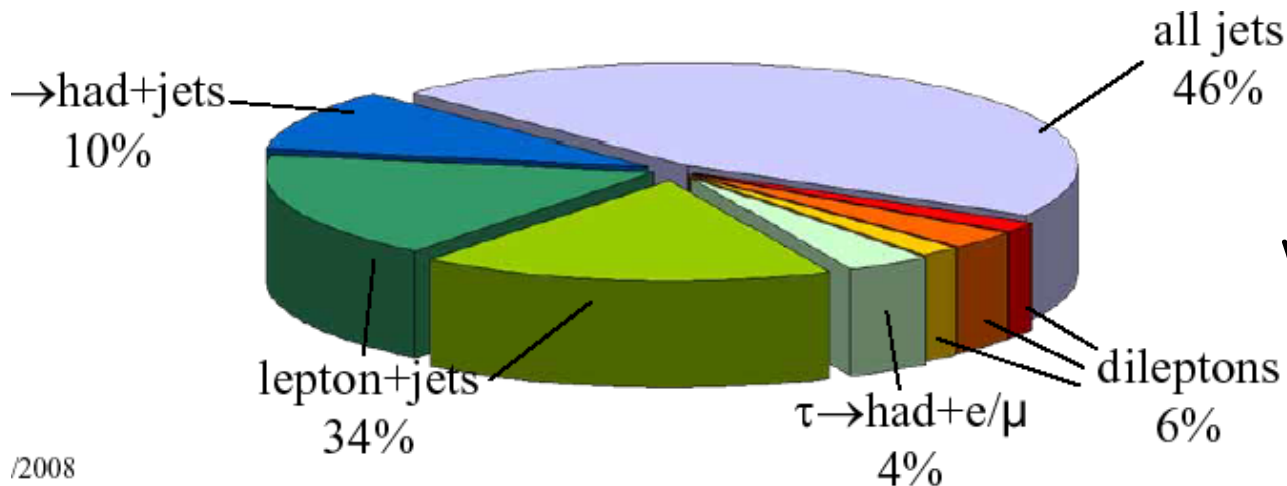
Identifying (tagging) the b -jets is important.



$$t \rightarrow W + b \text{ with } W \rightarrow l + \nu \text{ or } q + \bar{q} \rightarrow jet_1 + jet_2$$

$$\therefore t + \bar{t} \rightarrow W^+ + b + W^- + \bar{b}$$

Leads to: $l + \nu + 4 jets$ or $2l + 2\nu + 2 jets$ or $4 jets$



Are there any backgrounds?

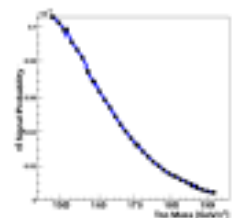
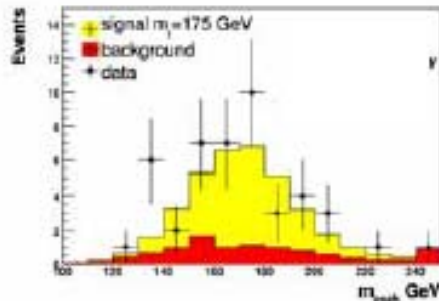
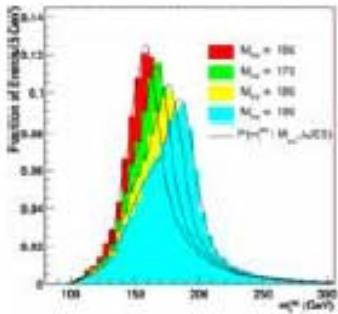
What backgrounds?



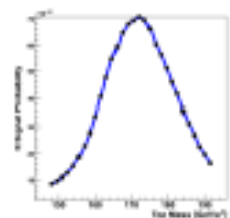
Top Mass Measurement

Template fitting: MC prod'n and decay for a given top mass yields templates. Then mathematically compare the simulated tt events and bkg to the data.

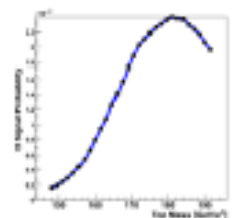
For each observed event assume a top mass and calculate the matrix element for the assumed top mass. Increment the top mass and calc. again. Generate prob. for each mass and find the joint prob. for the obsvd sample of events. Include bkgd.



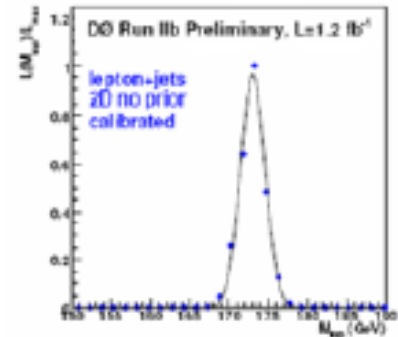
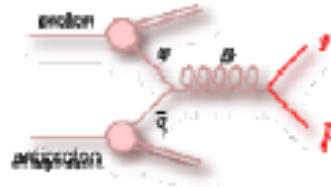
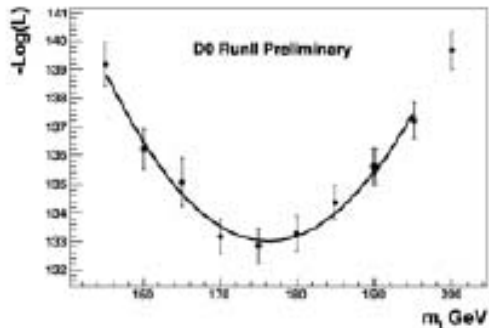
Event 1



Event 2



Event 3





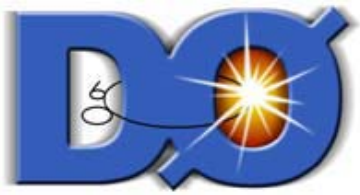
Lepton + jets: Selection, bkgd,

The lepton plus jets sample is well suited for the top mass determination. The branching fraction of $\sim 38\%$ and the lepton signature plus large missing E_T leads to a good sample for the top mass measurement. In the most recently analyzed sample there are **312 (303) e plus jets (μ plus jets)**.

Main Background: W + jets production is the largest contributor to background.

Tagging the two b-jets per top pair is important. If one cannot identify the b-jets then it is necessary to consider the various permutations of jets in identifying the two jets from a W decay. The **Tagging of b-jets** is possible by identifying a muon from one of the jets, or by measuring the decay vertex of the b-state as being distinct from the production vertex (a few mm).

In addition to measuring the top mass with this sample, it has been useful to check the **JES** by reconstructing the W mass from the jet decays of the u-dbar or c-bbar jets. The **JES** check using W jets agrees with the external calibration to better than 2%.



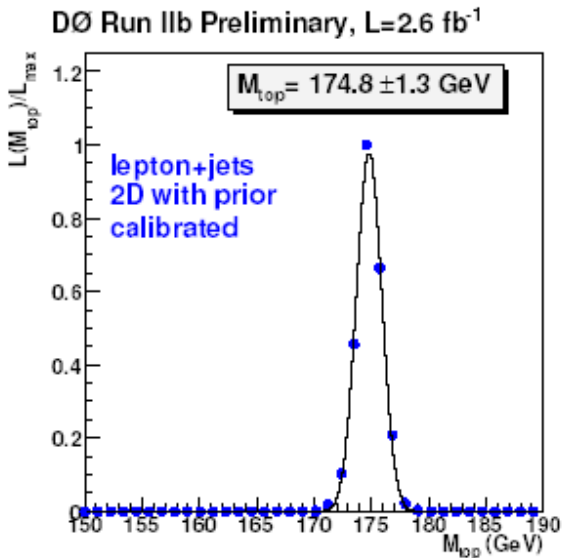
Lepton + Jets Matrix Element

3.6 fb⁻¹ - NN b-tagging.
 Matrix elements for both
 for Top and background.
 Use all meas'd kinematic
 information. Extract:

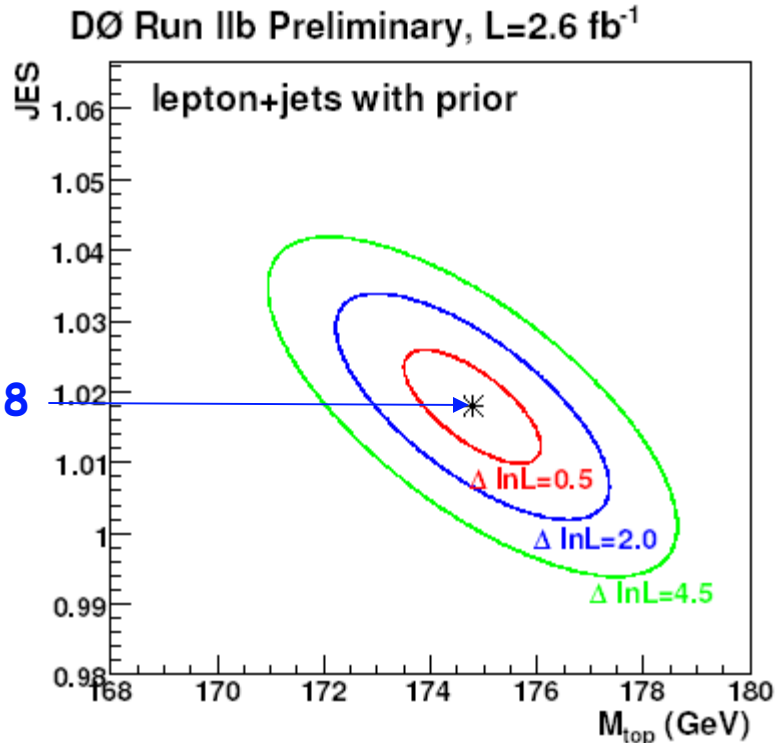
- Top mass
- Jet Energy scale

$$P(x; m_{top}) = \frac{1}{\sigma_{obs}(q\bar{q} \rightarrow t\bar{t} \rightarrow e\mu; m_{top})}$$

$$\int_{q_1, q_2, y} \sum_f dq_1 dq_2 f(q_1) f(q_2) \frac{|M|^2}{\sqrt{(q_1 \cdot q_2)^2}} \cdot d\Phi_6 \cdot W(x, y)$$



JES = 1.018





Top Mass: Dilepton Events

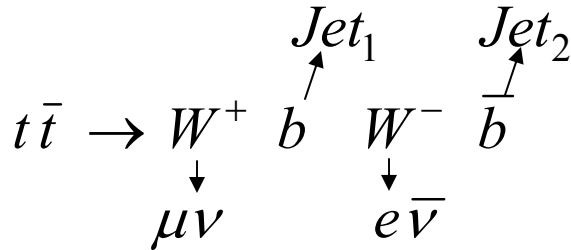
Run IIa 1.1 fb⁻¹ Run IIb 2.5 fb⁻¹

Event Selection:

e: $p_T > 15 \text{ GeV}$ $|\eta| < 1.1$ or $1.5 < |\eta| < 2.5$

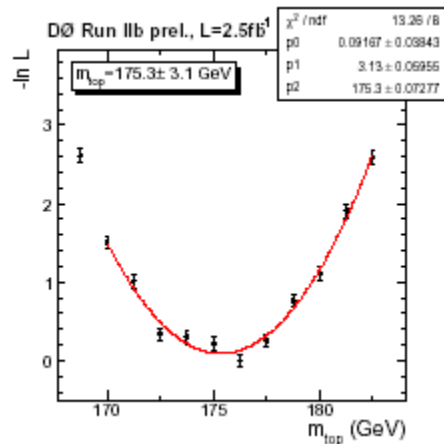
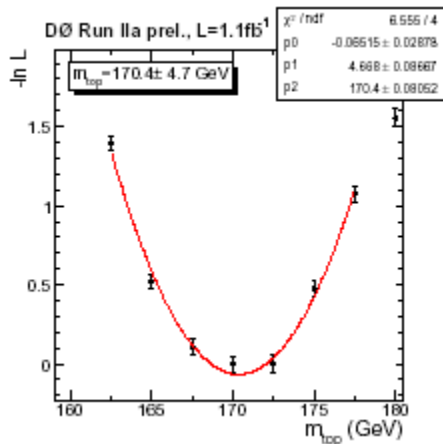
m: $p_T > 15 \text{ GeV}$ $|\eta| < 2$

2 jets w/ $p_T > 20 \text{ GeV}$, $|\eta| < 2.5$



Expected and Observed Events

	$t\bar{t} \rightarrow e\mu$	$Z \rightarrow \tau\tau \rightarrow e\mu$	WW/WZ	Fake e	Fake μ	Total	Obsvd
Run IIa	36.8±3.	6.0±1.0	1.6±0.4	0.8±0.3	1.9±0.5	46.9±3.5	39
Run IIb	81.7±0.3	3.8±0.8	4.4±0.4	2.6±0.7	2.1±0.9	94.5±1.4	115



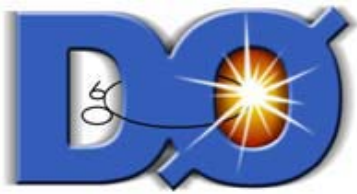
Combining the likelihood functions for

Runs II a and b gives

$$M_{e\mu}(\text{top}) = 174.8 \pm 3.3(\text{stat}) \pm 2.6 \text{ GeV or } = 174.8 \pm 4.2 \text{ GeV}$$

This $e\mu$ result has been combined with the ($\ell + \text{track}$ channel) to give:

$$M_{\ell\ell}(\text{top}) = 174.7 \pm 2.9(\text{stat}) \pm 2.4 \text{ GeV or } = 174.7 \pm 3.8 \text{ GeV } (\ell\ell)$$



Top Mass: $\ell + \text{jets}, \ell\ell + \text{jets}$

3.6 fb⁻¹

$$m_{top}^{\ell+\text{jets}} = 173.7 \pm 0.8(\text{stat}) \pm 1.6(\text{syst}) \text{ GeV} \text{ or}$$

$$m_{top}^{\ell+\text{jets}} = 173.7 \pm 1.8 \text{ GeV}$$

Run II a, b: $\ell + \text{jets}$

$$\chi^2 = 2.5 \text{ for } 1 \text{ d.o.f.}$$

3.6 fb⁻¹ $e\mu +$
1.0 fb⁻¹ $ee, \mu\mu$ &
0.13 fb⁻¹ $\ell + \text{trk}$

$$m_{top}^{\ell\ell} = 174.7 \pm 2.9(\text{stat}) \pm 2.4(\text{syst}) \text{ GeV} \text{ or}$$

$$m_{top}^{\ell\ell} = 174.7 \pm 3.8 \text{ GeV}$$

Run II a,b: ($\ell\ell$), Run I ($ee, \mu\mu, \ell/\text{tr}$)

Combining all Run I and Run II measurements yields:

$$m_{top} = 174.2 \pm 0.9(\text{stat}) \pm 1.5(\text{syst}) \text{ GeV} \text{ or}$$

$$m_{top} = 174.2 \pm 1.7 \text{ GeV}$$

T
h
e

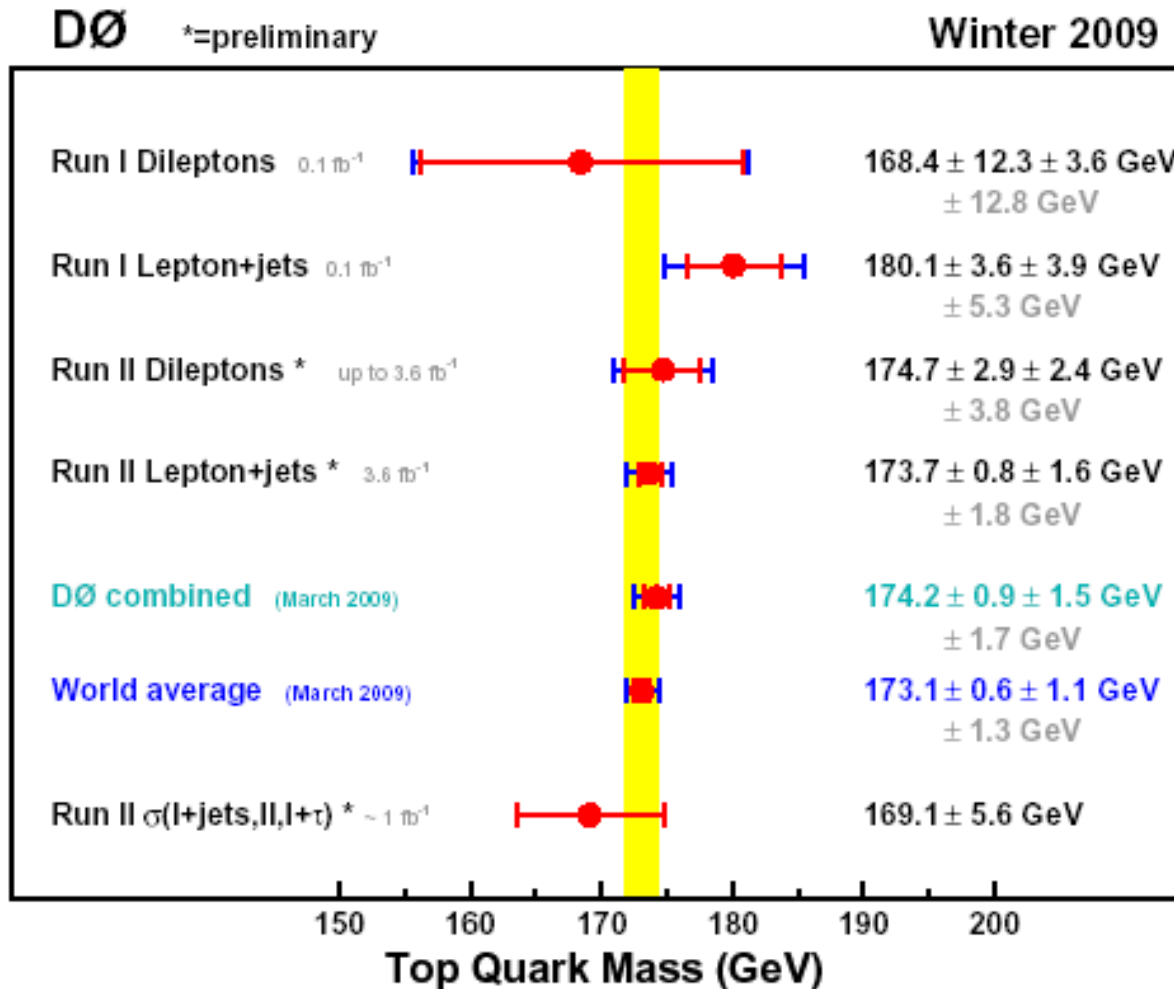
L. Lyons, D. Gibaut and P. Clifford, NIM A270, 110 (1988); A. Valassi, NIM A500, 391 (2003)

Summary of Weights of the Individual Measurements

	Run I		Run II				
	$\ell + \text{jets}$	$\ell\ell$	$\ell + \text{jets}$ Run IIa	$\ell + \text{jets}$ Run IIb	$e\mu$ Run IIa	$e\mu$ Run IIb	$ee, \mu\mu,$ $\ell + \text{trk}, \text{IIa}$
Weight	8.24%	0.78%	29.14%	64.19%	-0.51%	-3.44%	0.88%



Top Quark Mass History



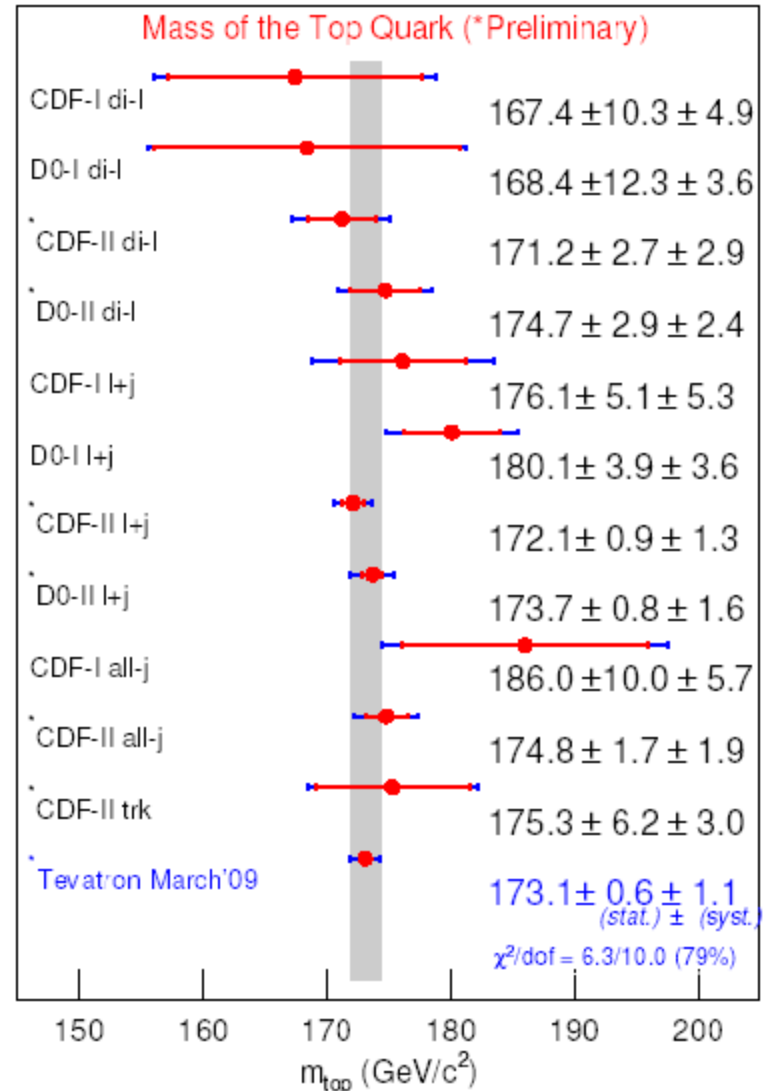


'09 Combined Top Mass: CDF/DØ

Tevatron Electroweak Working Group:
<http://tevewwg.fnal.gov> - Best Linear Unbiased Estimator (

Uncertainty Categories:

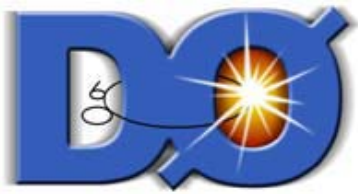
1. Statistical.
 2. Jet Energy Scale: W to qq'(in situ), jet flavor response, modeling of b-jets, tagging, light q vs. heavy q, out-of-cone cor., calibration issues, η -dependence, ..
 3. Trk based analysis.
 4. Signal modeling incl. across experiments.
 5. Background sources: QCD multi-jet, D-Y for dileptons, W+jets.
 6. Fitting and finite MC statistics.
 7. Monte Carlo: PYTHIA, ISAJET, HERWIG when modeling tt signal.
 8. U noise and multiple interactions.
 9. Color Reconnection.
 10. Multiple Hadron Interactions.
- Many correlations taken into account.



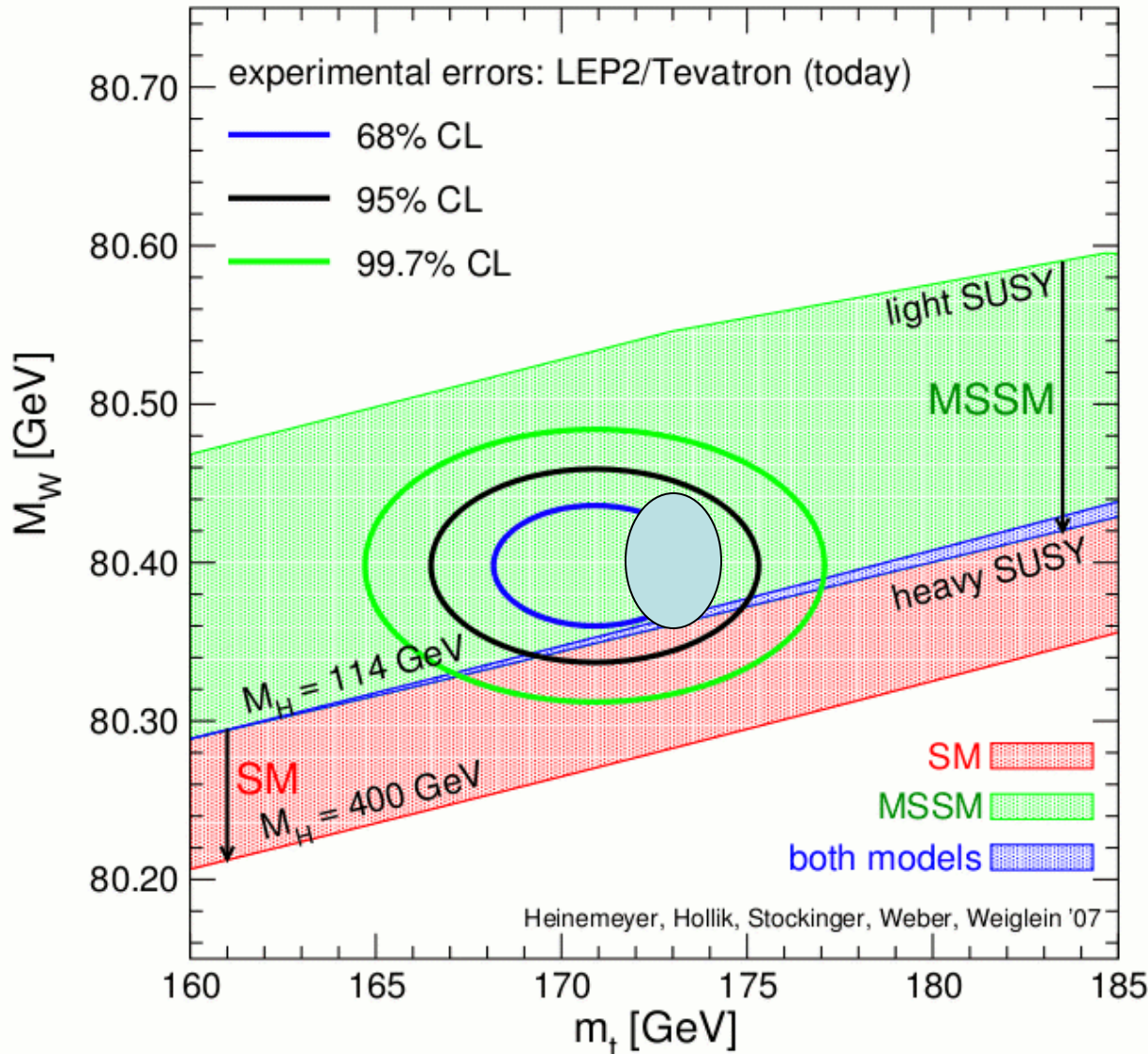
$$M_{\text{top}} = 173.1 \pm 0.6 \text{ (stat)} \pm 1.1 \text{ (syst)}$$

$$= 173.1 \pm 1.3 \text{ GeV}$$

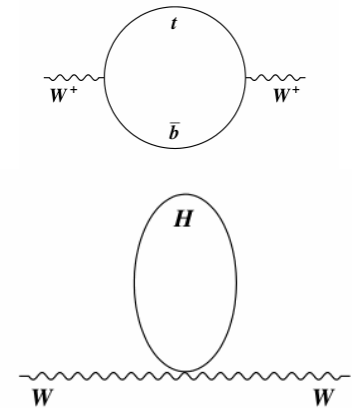
$$M_{\text{top}}(\text{2004}) = 174.3 \pm 5.1 \text{ GeV}$$



W Mass Measurement - 1fb⁻¹



$$M_W = \sqrt{\frac{\pi\alpha}{\sqrt{2}G_F \sin\theta_W}} \frac{1}{\sqrt{1-\Delta r}}$$



$$\Delta r = f(M_t^2, \log M_H)$$

If $\Delta M_t = 1.3$ GeV/c², need $\Delta M_W = 8$ MeV/c²,
 to make equal contributions to the Higgs mass.

2007 CDF (200pb⁻¹)
 $M_W = 80413 \pm 48$ MeV
 World Avg = 80398 ± 25 MeV



DØ b-Physics: CPV in B_s Decays?

DØ: PRL 101 241801 (2008)

Measurement of B_s mixing parameters from the Flavor-Tagged $B_s J/\psi \phi$ \longrightarrow

CDF: T. Aaltonen et al PRL 100 1618029 (2008).

Possible evidence that ϕ_s is larger than SM expectations A. Lenz & U. Nierste, JHEP 06,072 (2007). $\phi_s(\text{SM}) = (4.2 \pm 1.4) \times 10^{-3}$. Other decay modes?

New: [arXiv:0904.3907v1](https://arxiv.org/abs/0904.3907v1) Search for CP violation in semi-leptonic B_s decays. 5 fb^{-1} of data.

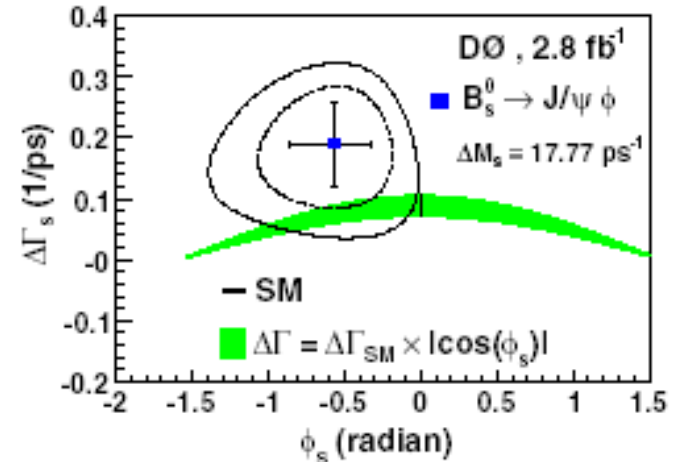
Event Sample:

$B_s \rightarrow \mu^+ D_s^- X$ with $D_s^- \rightarrow \phi \pi^-$ and $\phi \rightarrow K^+ K^-$ and

$B_s \rightarrow \mu^+ D_s^- X$ with $D_s^- \rightarrow K^{*0} K^-$ with $K^{*0} \rightarrow K^+ \pi^-$.

Flavor-specific asymmetry:

$$a_{fs}^s = \frac{\Gamma_{B^0(t) \rightarrow f} - \Gamma_{B^0(t) \rightarrow \bar{f}}}{\Gamma_{B^0(t) \rightarrow f} + \Gamma_{B^0(t) \rightarrow \bar{f}}} = \frac{\Delta\Gamma_s}{\Delta m_s} \tan \phi_s \quad (1a, 1b)$$



$B_s \rightarrow J/\psi \phi \rightarrow \mu^+ \mu^- K^+ K^-$

Using the world average values of $\Delta\Gamma_s$ and Δm_s that HFAG has determined, DØ calculates that:

$$a_{fs}^s = (-8.4_{-6.7}^{+5.2}) \times 10^{-3}$$

This can be compared to the SM expectation:

$$= (0.0206 \pm 0.0057) \times 10^{-3}$$



Search for CPV in B_s Decay

No angular analysis is needed; All production and decay information is used.

Likelihood Ratio used in selecting B_s candidates:

1. Helicity angle between D_s and K^\pm momenta in the ϕ or K^{*0} CM;
2. Isolation of the $\mu+D_s$ system;
3. χ^2 of the D_s vertex;
4. Invariant mass limits for:
 $(\mu+D_s)$, (K^+K^-) in the $\mu\phi\pi^-$ sample,
 $(K^+\pi^-)$ in the $\mu^+K^{*0}K^-$ sample.
5. $p_T(K^+K^-)$ in the $\mu\phi\pi^-$ sample,
 $p_T(K^-)$ in the $\mu^+K^{*0}K^-$ sample.

Maximize the $S/\sqrt{(S+B)}$ $S = \text{sig}$, $B = \text{bkg}$
 D_s candidates satisfying the reqs are:

$N(\mu\phi\pi) = 81,394 \pm 865$ and the
 $N(\mu K^*K) = 33,557 \pm 1,200$.

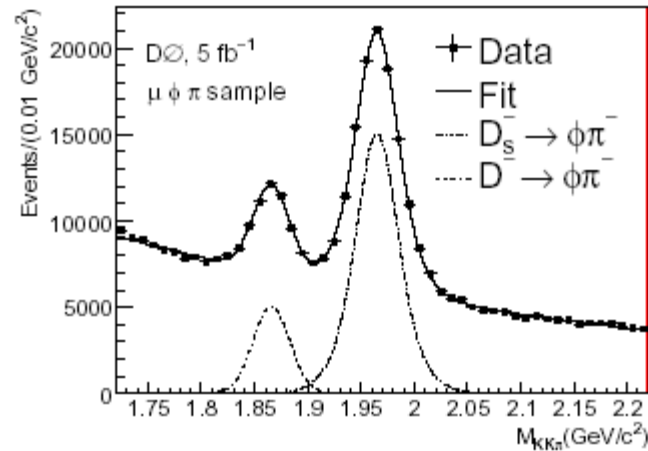


FIG. 1: $K^+K^-\pi^-$ invariant mass distribution for the $\mu^+\phi\pi^-$ sample with the curves representing the mass fit results.

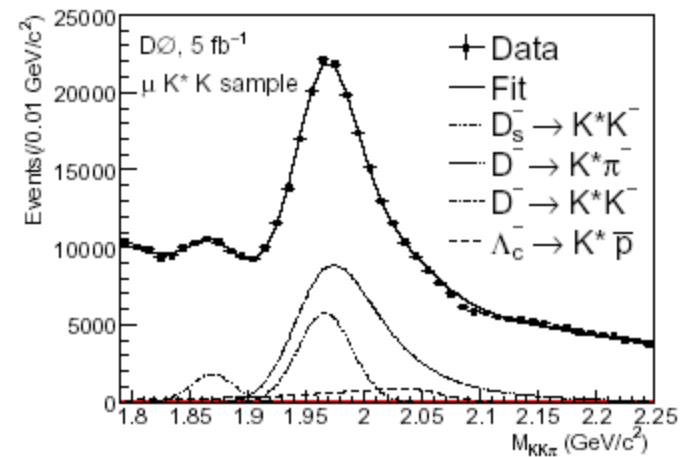
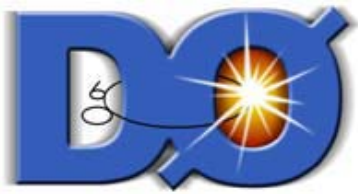


FIG. 2: $K^+K^-\pi^-$ invariant mass distributions for the $\mu^+K^{*0}K^-$ sample with the curves representing the mass fit results.



Search for CPV in B_s Decay

We want to measure an asymmetry that is expected to be very small in the SM. extreme care must be taken. We cannot allow our detector to introduce bias nor can our methods of analysis. We have been through a similar study using dimuons and there learned how to measure possible detector charge asymmetries:

$$A_\mu = (1 + qA_q)(1 + \gamma A_{\text{det}})(1 + q\beta\gamma A_{\text{ro}}) \cdot (1 + q\gamma A_{\text{fb}})(1 + \beta\gamma A_{\beta\gamma})(1 + q\beta A_{q\beta}),$$

β is the toroid polarity, γ is the sign of the muon pseudorapidity (+1 for $\eta > 0$), and q is the muon charge. The muon reconstruction asymmetry was measured using a $J/\psi \rightarrow \mu^+ \mu^-$ sample which gave: $A_q = (-1.90 \pm 0.45) \times 10^{-3}$. A_{fb} is the forward-backward asymmetry; A_{det} is detector η asymmetry, A_{ro} is the range-out asymmetry, $A_{q\beta}$ is a detector asymmetry between tracks bending to/away from $\eta < 0$.

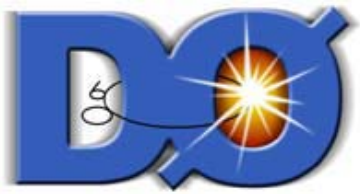
TABLE I: Asymmetries with statistical uncertainties.

	$\mu^+ \phi \pi^-$	$\mu^+ K^{*0} K^-$	Combined
$a_{fs}^s \times 10^3$	-7.0 ± 9.9	20.3 ± 24.9	-1.7 ± 9.1
$a_{fs}^d \times 10^3$	-21.4 ± 36.3	50.1 ± 19.5	40.5 ± 16.5
$a_{bg} \times 10^3$	-2.2 ± 10.6	-0.1 ± 13.5	-3.1 ± 8.3
$A_{\text{fb}} \times 10^3$	-1.8 ± 1.5	-2.0 ± 1.5	-1.9 ± 1.1
$A_{\text{det}} \times 10^3$	3.2 ± 1.5	3.1 ± 1.5	3.1 ± 1.1
$A_{\text{ro}} \times 10^3$	-36.7 ± 1.5	-30.2 ± 1.5	-33.3 ± 1.1
$A_{\beta\gamma} \times 10^3$	1.1 ± 1.5	0.2 ± 1.5	0.6 ± 1.1
$A_{q\beta} \times 10^3$	4.3 ± 1.5	2.0 ± 1.5	3.1 ± 1.1

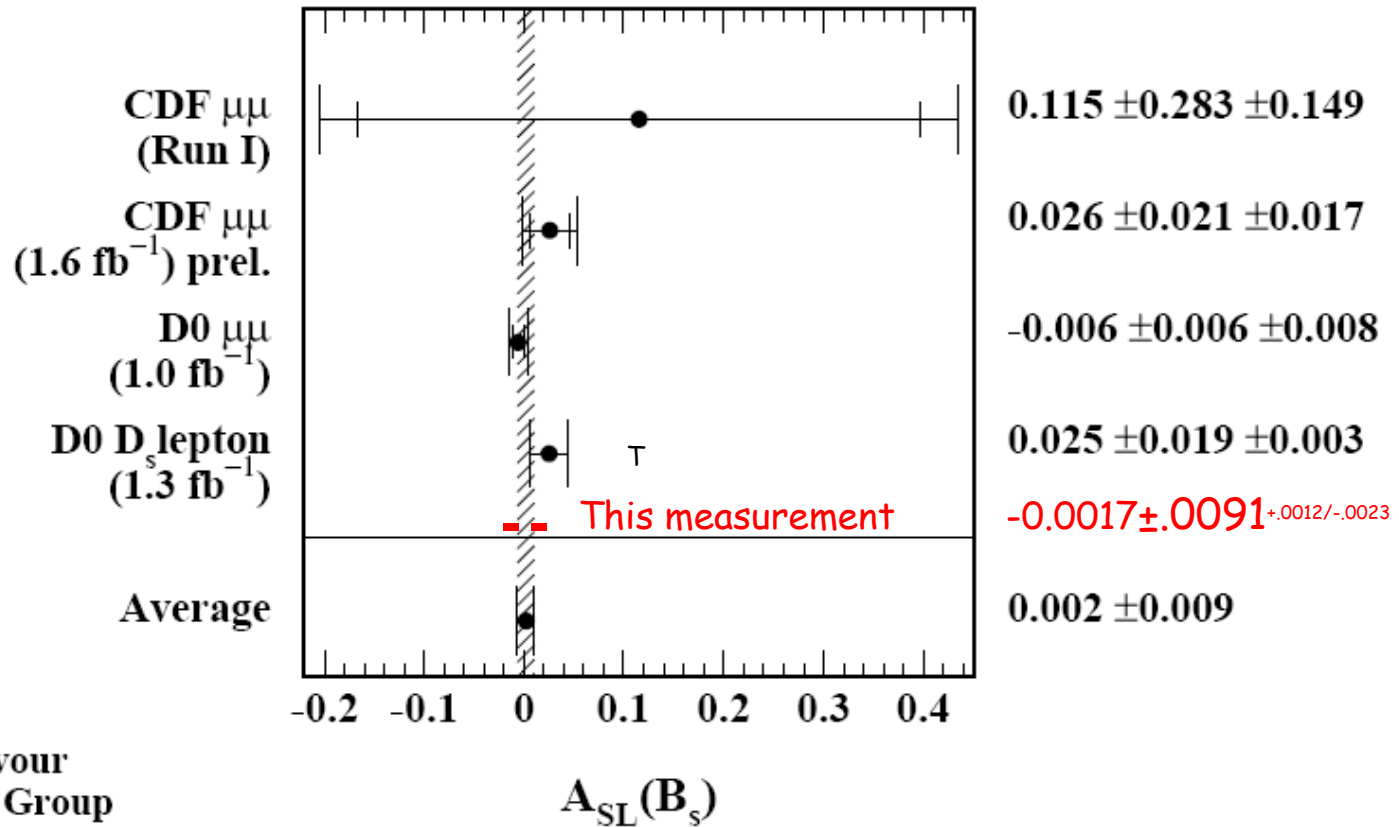
a_{bg} is a background asymmetry that is measured in the left and right sides of the mass peaks and then extrapolated in the mass regions.

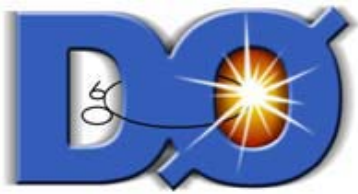
$A_{\beta\gamma}$ is a second-order correction to A_{ro} .

$a_{fs}(B_s) = (-1.7 \pm 9.1) \times 10^{-3}$, which is smaller than previous measurements by a factor of 2.



a_{sl}^S Summary





Search for the SM Higgs $\sim 2.7\text{fb}^{-1}$

Previous searches: D0 based on 0.17, 0.44 and 1.1fb^{-1} ; CDF on 0.32 and 0.95fb^{-1} .

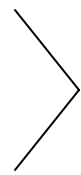
There are many searches in D0. We survey one of that covers the low mass and that demonstrates some of the approaches that are being taken: $W + H$. The production is $q + q' \rightarrow W H \rightarrow W b b$. (primary decay mode for low m_H)

So the final state is: $l \nu b \bar{b}$ where $l = e, \mu$ which means: lepton, missing E_T , two b jets. We trigger on both 2 and 3 jets. **jets**: (more Higgs and independent samples).

e or μ ,

missing E_T ,

2 or 3 jets.



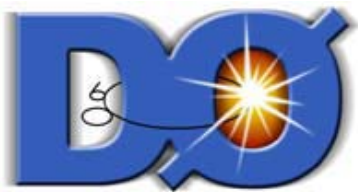
Classic $W + \text{jets}$, **with b-tags**.

The **backgrounds** are expected to be: for **two tags**: $W + b + \bar{b}$, $t + \bar{t}$, single t.

and for **one tag**: Multi-jets & W prod'n with c or light quarks.

The 3-jet and 2-jet sub-samples are separated into those with exactly "one tight" b-tagged jet and those with "two loose" b-tagged jets with no overlap.

A neural net (NN) algorithm that uses kinematics and matrix element calculations is applied to the events to obtain a discriminant that separates SM background from the signal by obtaining a high value of the discriminant.



Event Samples & Simulation

The triggers select e 's and μ 's with good efficiency, $\sim 90 - 95\%$, 70% , respectively, for analysis. To develop the NN algorithms and make quantitative comparisons of the events with theory, many reliable simulations were required for both backgrounds and signals.

The simulation data sets were also needed to choose the variables to include in the NN calculations and for comparisons with data; e.g. $W H \rightarrow \ell \nu b \bar{b}$, $\ell = e, \mu, \tau$

Simulated backgrounds include: diboson WW and WZ production (PYTHIA), W + jets and Z +jets (ALPEN & PYTHIA), single Top: s channel $t\bar{b}$ events, t channel $t\bar{b}g$ COMPHEP & PYTHIA.

MC yields from generated events were compared and renormalized relative to the data when required by as much as 30% in one instance.

Leptons used in the analyses were first defined with "loose" criteria that was subsequently tightened to become known as "tight" e 's or μ 's depending on quantitative measures such as what fraction of an electron's energy could reside in the (η, ϕ) conical section radius between 0.2 and 0.4 units. (ans. 15%)

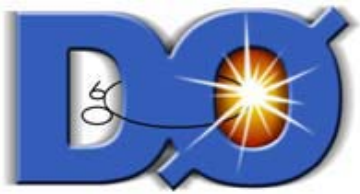


SM Backgrounds & b-tags

	$W + 2$ jets	$W + 2$ jets (1 b tag)	$W + 2$ jets (2 b tag)	$W + 3$ jets	$W + 3$ jets (1 b tag)	$W + 3$ jets (2 b tag)
WH, ZH	15.8 ± 2.7	6.8 ± 1.3	3.9 ± 0.7	3.8 ± 0.6	1.6 ± 0.3	1.0 ± 0.2
WW, WZ, ZZ	1453 ± 244	87 ± 16	13.7 ± 2.6	302 ± 51	23.1 ± 4.2	3.9 ± 0.7
$W/Z + b\bar{b}$	1769 ± 353	592 ± 109	138 ± 27	471 ± 94	174 ± 32	49.2 ± 9.4
$t\bar{t}$	581 ± 98	242 ± 45	96.9 ± 19	926 ± 155	394 ± 73	211 ± 41
Single top	290 ± 49	123 ± 23	31.5 ± 6.1	91 ± 15	38.5 ± 7.0	16.9 ± 3.2
Multijet	3575 ± 629	189 ± 38	16.7 ± 4.0	1228 ± 216	92.8 ± 18	14.4 ± 3.4
$W/Z +$ jets	44464 ± 570	942 ± 226	44.5 ± 9.8	8357 ± 105	239 ± 57	25.7 ± 5.8
Total expectation	52148 (n.t.d.)	2182 ± 348	345 ± 51	11379 (n.t.d.)	963 ± 152	322 ± 49
Observed Events	52148	2174	336	11379	912	321

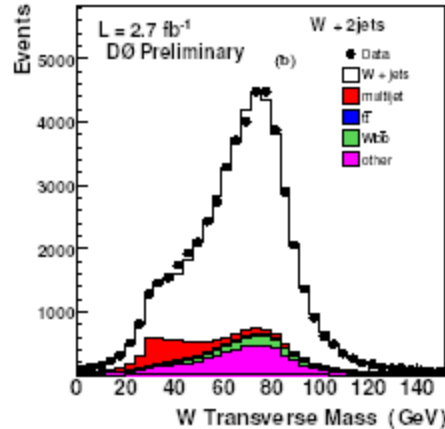
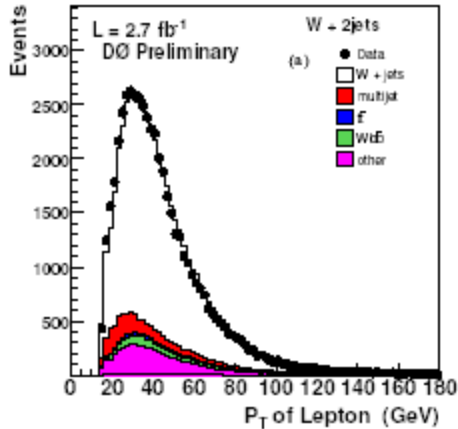
TABLE I: Summary table for the $W + 2,3$ jet final states. Observed events in data are compared to the expected number of $W +$ jet events before tagging, with exactly one tight b -tagged jet, and with exactly 2 loose b -tagged jets. First three columns are for the $W + 2$ jet channel, the last three columns for the $W + 3$ jet channel. Expectation originates from the simulation of WH and ZH (with $m_H = 115$ GeV), dibosons (WW, WZ, ZZ , labeled WZ in the table), $Wb\bar{b}$ production, top production ($t\bar{t}$ and single-top), multijet background and “ $W +$ jet” production, which contains light and c quarks. All Z processes are fully simulated, and included in the corresponding W categories. The processes $W(Z)b\bar{b}$ and $W(Z) +$ light and/or c jets are counted separately. “n.t.d.” stands for “normalized to data”. The uncertainties given include statistics and systematics.

DO's b -tagging was ultimately implemented by using a neural network algorithm. Seven variables were chosen to be those with the best discriminating power. These variables were shown to have direct sensitivity to the presence of tracks that separate the primary and secondary vertices. The efficiency for identifying a jet containing a b -hadron for the loose and tight operating points are about $59 \pm 1\%$ and $48 \pm 1\%$, respectively for a jet Pt of 50 GeV/c.



W + 2-jet Data & MC

Lepton P_T

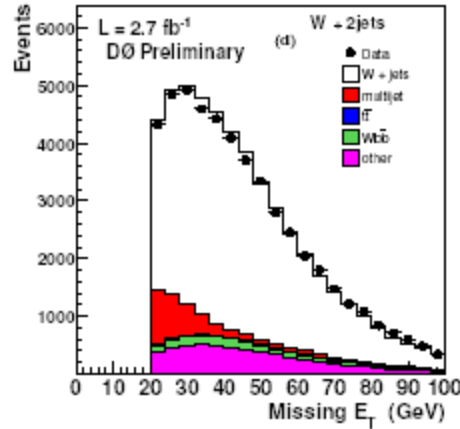
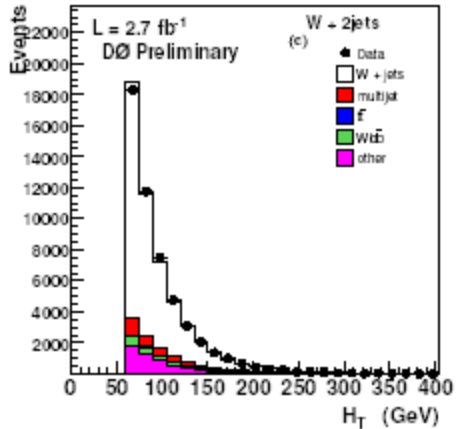


W Transverse Mass

$$M_T = \sqrt{2p_T^l p_T^v (1 - \cos(\phi_l - \phi_v))}$$

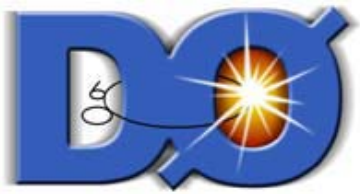
p_T^v = missing transverse energy

H_T = sum of $|p_{+}|$ of the jets.



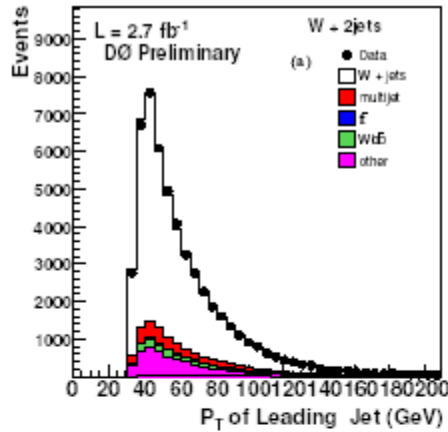
Missing E_T

FIG. 1: Distribution in the W + 2 jets sample of the (a) lepton momentum, (b) the transverse W mass, (c) the H_T variable and (d) missing transverse energy compared to the simulated expectation in the W + 2 jet event sample. The simulation is normalized to the integrated luminosity of the data sample using the expected cross sections (absolute normalization) except for the W + jets sample which is normalized on the "untagged sample" to the data, taking into account all the other backgrounds.

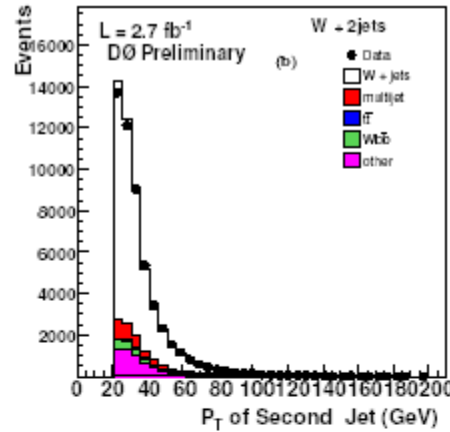


W + 2j: P_T , ΔR , m_{j_1, j_2}

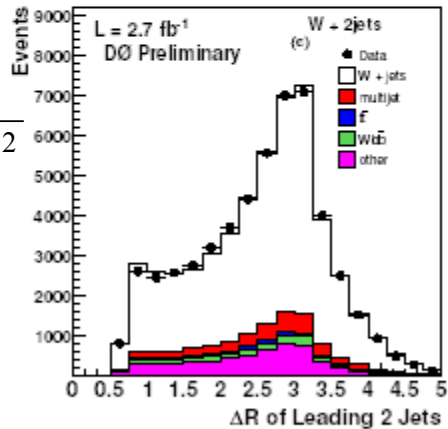
$P_T(J_1)$



$P_T(J_2)$



$$\Delta R = \sqrt{(\Delta\phi)^2 + (\Delta\eta)^2}$$



Di-jet Mass

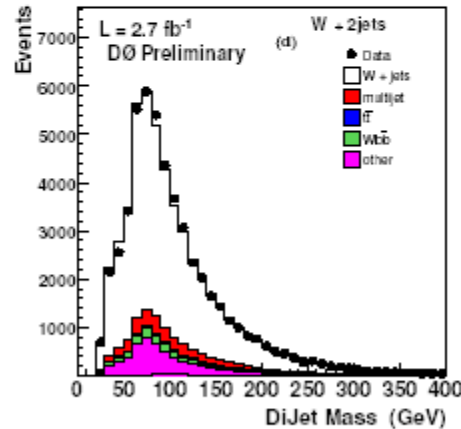
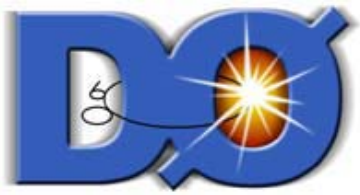
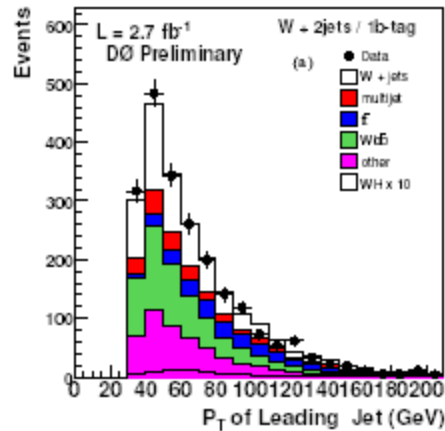


FIG. 2: Distribution in the W + 2 jets sample of the (a) p_T of the leading and (b) next to leading jet, (c) of the distance in the $\eta - \phi$ plane between the two jets and (d) of the dijet mass (d) between the two jets in the W + 2 jet sample compared with the simulated expectation. The simulation is normalized to the integrated luminosity of the data sample using the expected cross sections (absolute normalization) except for the W + jets sample which is normalized on the "untagged sample" to the data, taking into account all the other backgrounds.

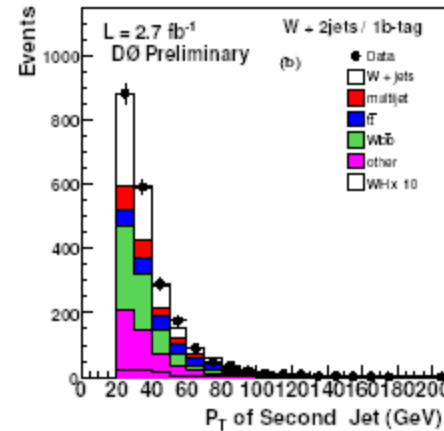


W + 2 jets - with 1 b-tag

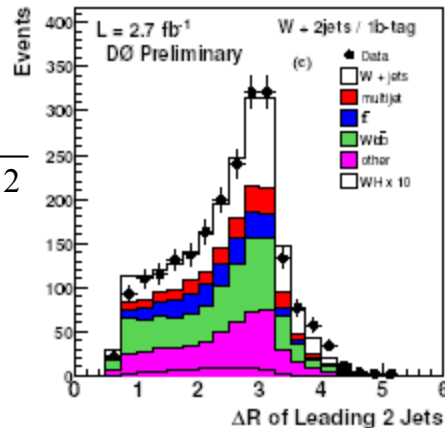
$P_T(J_1)$



$P_T(J_2)$



$$\Delta R = \sqrt{(\Delta\phi)^2 + (\Delta\eta)^2}$$



Di-jet mass

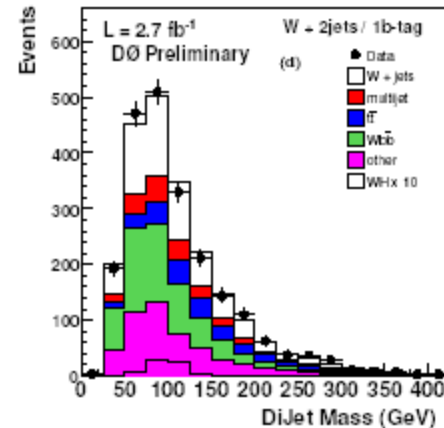
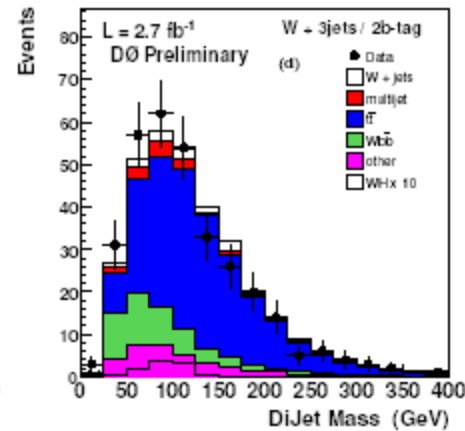
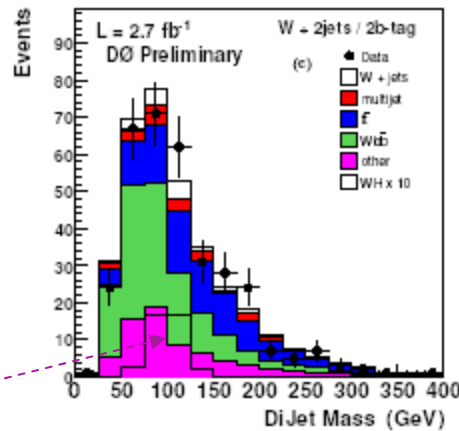
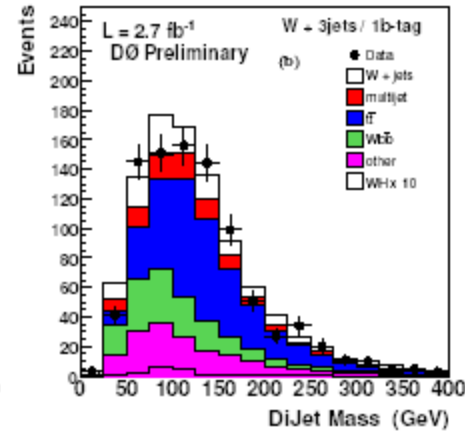
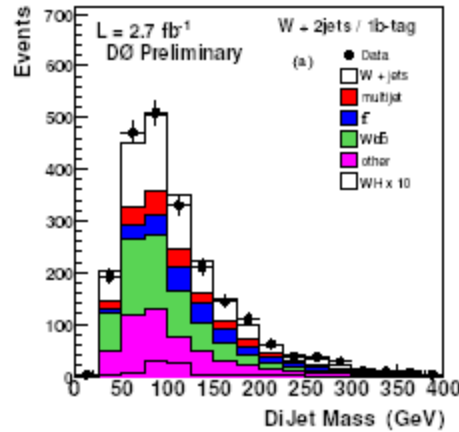


FIG. 3: Distribution in the W + 2 jets sample with one b-tagged jet of (a) the p_T of the leading and (b) next to leading jet, (c) of the distance in the $\eta - \phi$ plane between the two jets and (d) of the dijet mass between the two jets in the W + 2 jet sample compared with the simulated expectation. The simulation is normalized to the integrated luminosity of the data sample using the expected cross sections (absolute normalization) except for the W + jets sample which is normalized on the "untagged sample" to the data, taking into account all the other backgrounds. Also shown is the contribution expected for standard model WH production with $m_H = 115$ GeV, multiplied by a factor 10.



Di-jet Mass: $W+2j$ & $W+3j$ + tag(s)



$W+2jets/1$ b-tag

$W+3jets/1$ b-tag

$W+2jets/2$ b-tags

$W+3jets/2$ b-tags

Note: $WH \times 10$

FIG. 5: a) (b) dijet invariant mass in $W+2(3)$ jet events when exactly one jet is b-tagged. c) (d) same distributions when at least 2 jets are b-tagged. Linear scale. The simulated processes are normalized to the integrated luminosity of the data sample using the expected cross sections (absolute normalization) except for the $W+$ jets sample which is normalized on the "untagged sample" to the data, taking into account all the other backgrounds. The backgrounds labelled as "other" in the figure are dominated by single-top production. Also shown is the contribution expected for standard model WH production with $m_H = 115$ GeV, multiplied by a factor 10.



Higgs Search Neural Network (NN)

Optimize the search sensitivity in the $W+2j$ events using the difference in kinematic properties of the **lepton, two jets** and $E_T(\text{missing})$ in a NN that is trained on both WH signal MC events and the backgrounds shown in the previous plots:

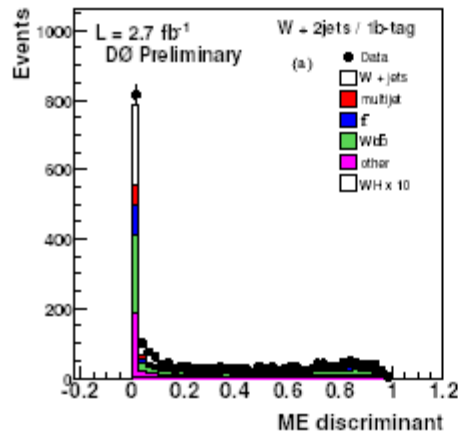
1. p_T of the leading jet;
2. p_T of the 2nd jet;
3. $\Delta R = \sqrt{(\Delta\eta)^2 + (\Delta\phi)^2}$ between the two jets;
4. $|\Delta\phi|$ between the two jets;
5. p_T of the dijet system;
6. dijet invariant mass; ← Best $W+2j$ discriminant - Use it as the final discriminant for $W+3j$ event sample.
7. p_T (lepton, $E_T(\text{miss})$) system;
8. Matrix Element discriminant

The ME discriminant uses 4-vectors for the lepton and 2 jets and integrates over the unmeasured momentum of the ν convoluting it with the resolution for the detector to calculate the relative probability for WH vs. backgrounds. Then the ME prob. goes into the NN. NN training is done for 8 channels: $(e, \mu) * (ST, DT) * (\text{Run IIa}, \text{Run IIb})$. Separate training is done for each assumed Higgs mass. $m_H = 115\text{GeV}$ in the plots.

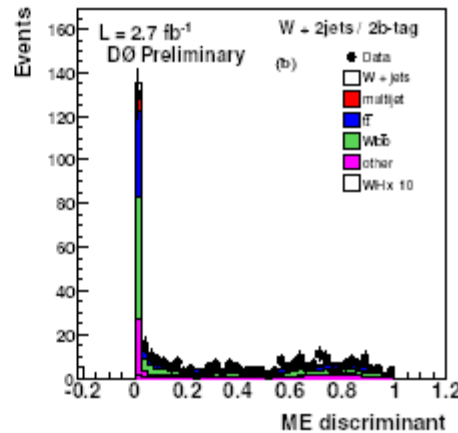


W+2j with 1 or 2 b-tags + ME

W+2jets/1 b-tag

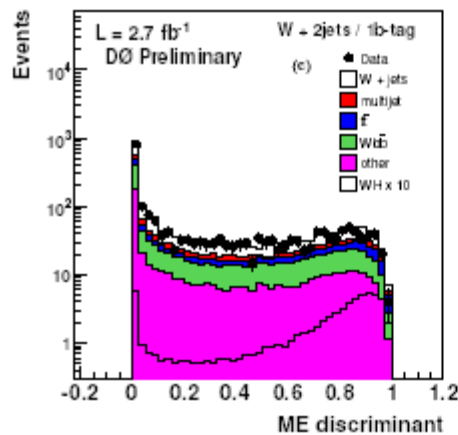


W+2jets/2 b-tags

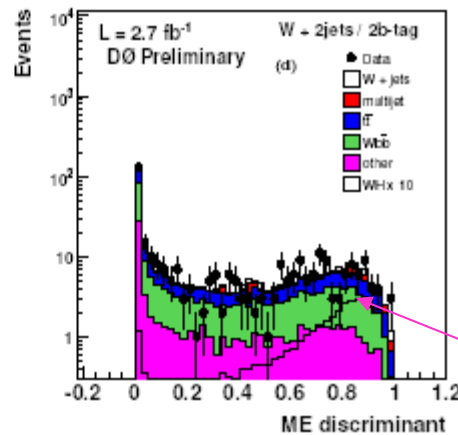


Ln plot

W+2jets/1 b-tag

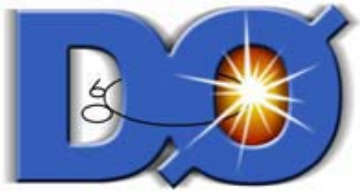


W+2jets/2 b-tags



ME disc shows upturn at large values as expected.

FIG. 7: Distributions of the Matrix Element discriminant compared with the simulated expectation: a) in the single b -tag sample for the single-tag ME discriminant; b) in the double b -tag sample for the double-tag ME discriminant; c) log scale of figure (a); d) log scale of figure (b); The simulation is normalized to the integrated luminosity of the data sample using the expected cross sections (absolute normalization) except for the W +jets sample which is normalized on the "pre-tag sample" to the data, taking into account all the other backgrounds. The WH expected contribution which is scaled by a factor 10 is peaking at high values of the ME discriminant as shown in c) and d).

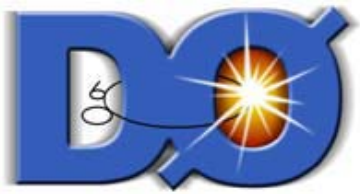


Cross Section Limit for Higgs Prod'n

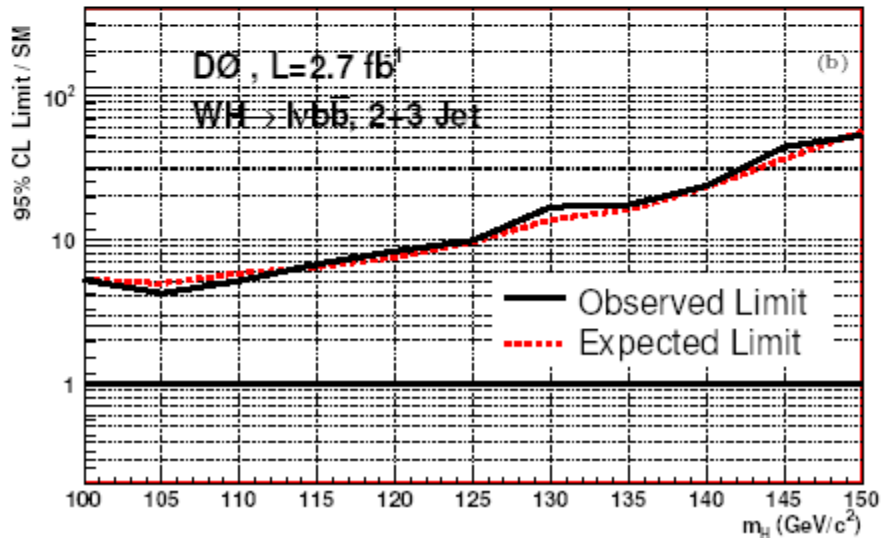
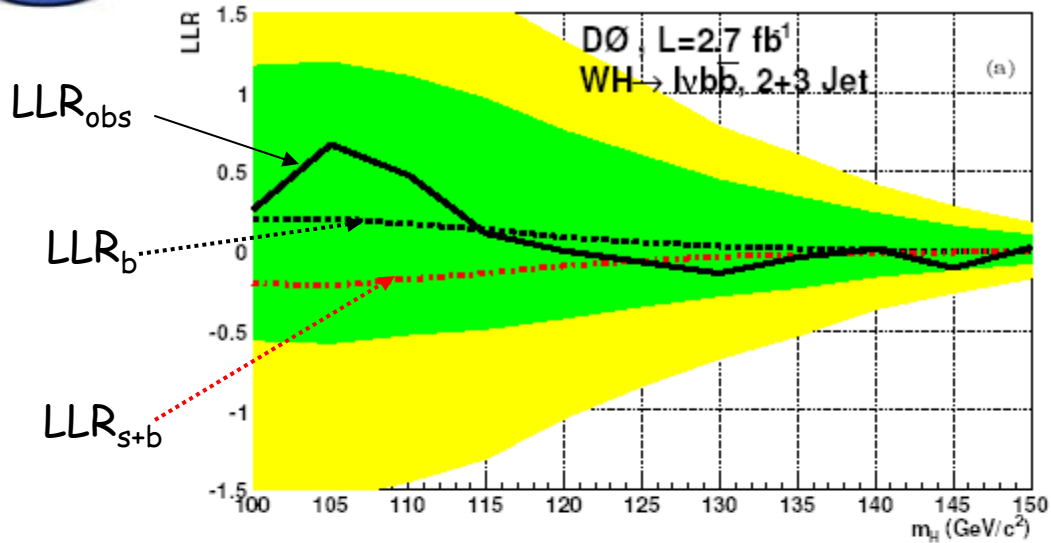
Our previous plots show data and MC expectations for a Higgs of mass 115 GeV, produced in association with a W, for ST W+2 or 3j and for DT W+2 or 3j. Since no excess is seen, we can set limits on the Higgs cross section using the NN output For W+2j and the dijet mass discriminant for W+3j data.

Each channel is analyzed independently (e, μ), (ST, DT), (W+2j, W+3j), (Run IIa, IIb) and then all 16 channels are combined. The 95% CL (modified frequentist) method is used with a Poisson log-likelihood ratio (LLR) test statistic.

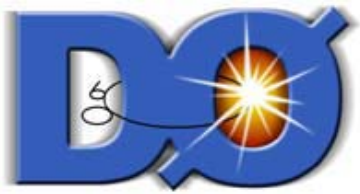
Log likelihood ratios (LLR) follow for the signal + background hypothesis: LLR_{s+b} , background only LLR_b and the observed data LLR_{osv} .



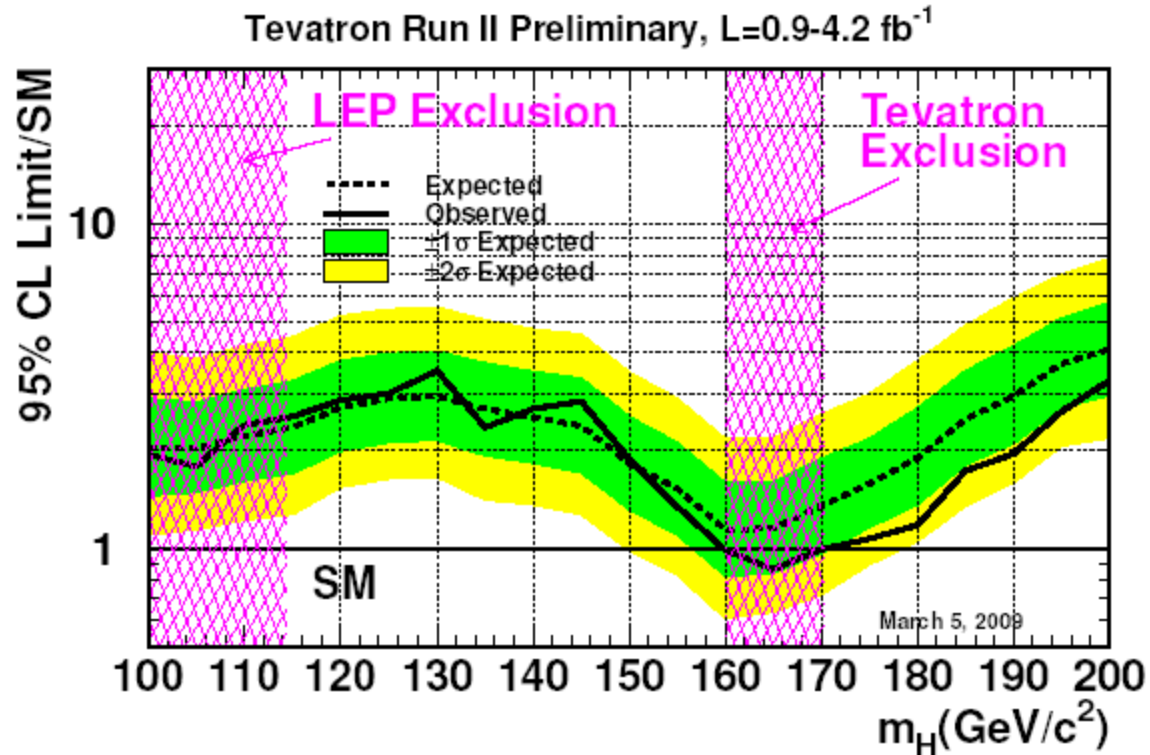
Higgs Cross Section 2.7fb^{-1}



The cross section limit for:
 $\sigma(pp \rightarrow WH) \times$
 $BR(H \rightarrow bb)$ is $6.7 \times$
the SM expectation
for $m_H = 115 \text{ GeV}$ at
95% CL.



DO/CDF combined Higgs mass limits





Summary/Conclusions

The Tevatron, D0 and CDF have reached significant milestones in recent years!

Record luminosities and many other operational records.

Physics results on:

Inclusive jet cross section 7 years in the making.

Preliminary new D0 W mass: $80.401 \pm 0.021(\text{stat.}) \pm 0.038(\text{syst.}) \text{ GeV}$
LAr plus inventive colleagues!

Top mass of $173.1 \pm 1.3 \text{ GeV}$ D0 & CDF comb nearing publication.

Soon to have a new M_{top} vs. M_w plot.

Interesting progress on measuring B_s mixing and searches for CPV in the B_s system.

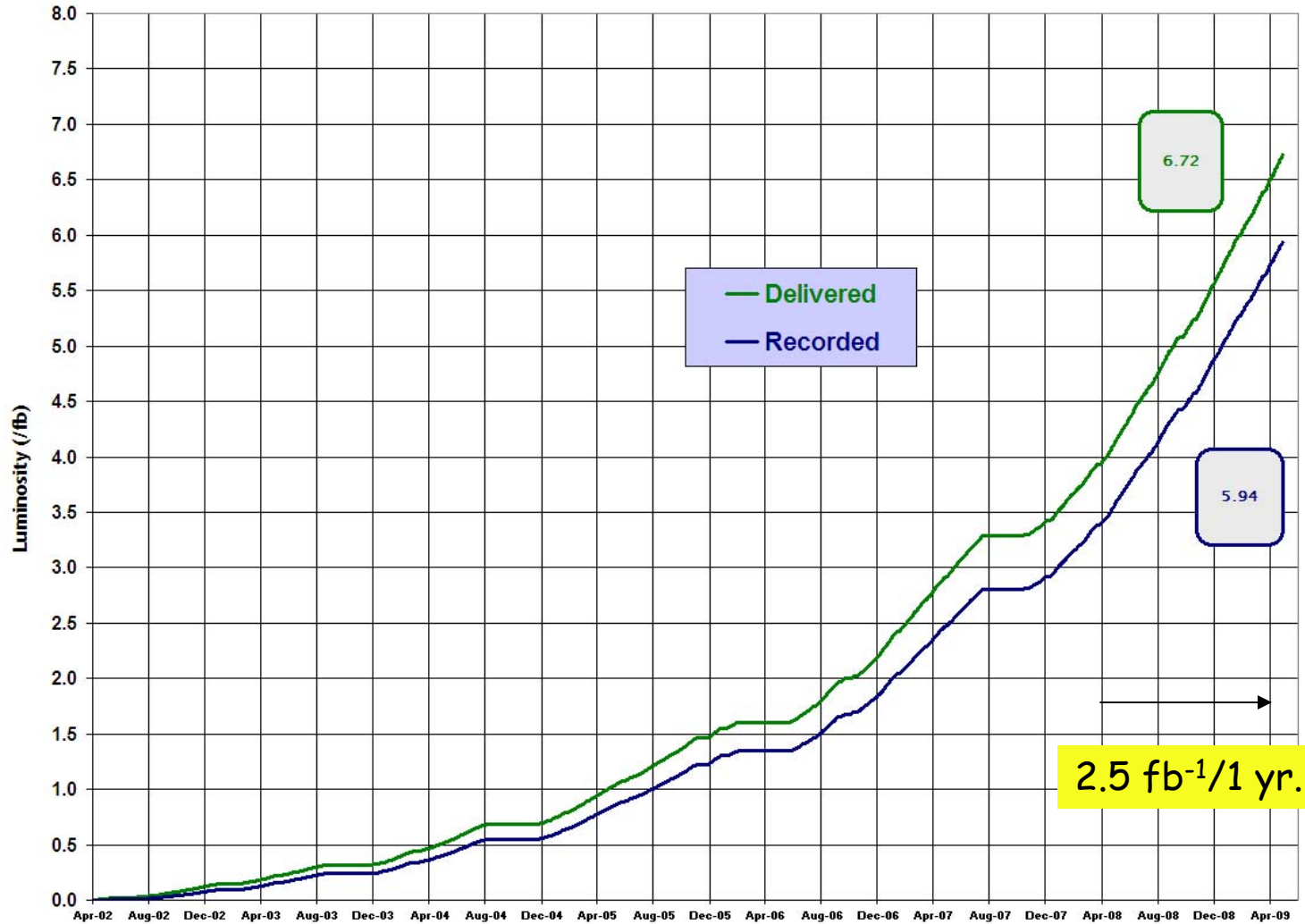
Higgs mass region is being narrowed by CDF and D0.

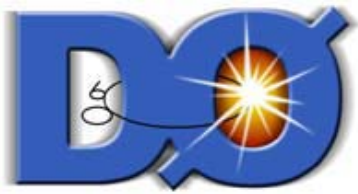
More to follow.



Run II Integrated Luminosity

19 April 2002 - 17 May 2009





Di-jet Mass: $W+2j$ & $W+3j$ + tag(s)

Ln plots

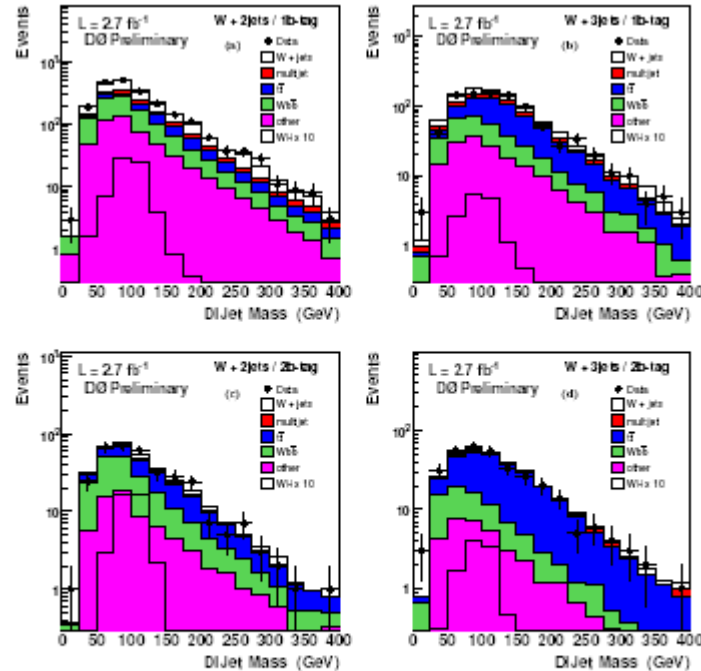


FIG. 6: a) b) dijet invariant mass in $W+2(3)$ jet events when exactly one jet is b-tagged. c) d) same distributions when at least 2 jets are b-tagged. Logarithmic scale. The simulated processes are normalized to the integrated luminosity of the data sample using the expected cross sections (absolute normalization) except for the $W+ jets$ sample which is normalized on the "antitagged sample" to the data, taking into account all the other backgrounds. The background labeled as "other" in the figure are dominated by single-top production. Also shown is the contribution expected for standard model WH production with $m_H = 115$ GeV, multiplied by a factor 10.